NUCLEAR MAGNETIC RESONANCE RELAXATION TIME IN CH_2I_2

by

HARTWIG PEEMOELLER

B.Sc., University of Winnipeg, 1969

A THESIS SUBMITTED IN PARTIAL FULFILLMENT

OF THE REQUIREMENTS FOR THE DEGREE OF

MASTER OF SCIENCE

in the Department

of

Physics

ACCEPTED

FACULTY OF GRADUATE STUDIES

[redacted]

Assoc. DEAN

DATE 2 May 74

We accept this thesis as conforming
to the required standard

[redacted]

UNIVERSITY OF VICTORIA

APRIL 1974

Supervisor: Dr. H.S. Sandhu

ABSTRACT

Measurements of spin-lattice relaxation time, T_1, of protons in oxygen-free samples of 100% CH_2I_2, 80% CH_2I_2 - 20% CD_2I_2 , 60% CH_2I_2 - 40% CD_2I_2, 40% CH_2I_2 - 60% CD_2I_2 and of deuterons in oxygen-free samples of CD_2I_2 have been carried out between 7 - 100°C at a frequency of 4 Mc/sec using pulse techniques.

The intermolecular dipole-dipole, intramolecular dipole-dipole and spin-rotational contributions have been separated. The results show that both the intramolecular dipole-dipole and intermolecular dipole-dipole contributions are temperature dependent and the intramolecular dipole-dipole interaction is predominant in causing relaxation. The contributions due to intramolecular dipole-dipole and intermolecular dipole-dipole interactions are found to be 67.5% and 32.5% of the total relaxation respectively between 7 - 100°C. The intra- and intermolecular dipole-dipole contributions due to interactions between non-identical spins are 5% of the intramolecular dipole-dipole contribution and 24% of the intermolecular dipole-dipole contribution respectively. The spin-rotational contribution is zero over the temperature range studied. The intermolecular dipole-dipole contribution calculated using the

Bloembergen, Purcell and Pound theory, modified by Gierer and Wirtz to take into account the finite size of the molecules, agrees with the experimental value to within 22%. The activation energies of the intramolecular dipole-dipole and intermolecular dipole-dipole contributions are 3.14 ± 0.03 kcal/mole and 3.13 ± 0.03 kcal/mole respectively. The activation energy obtained from the deuteron T_1 data is 3.07 ± 0.02 kcal/mole.

The rotational motion of this molecule appears to be anisotropic and the microviscosity theory for rotational diffusion seems to apply here. The rotational correlation times calculated from the Debye - BPP expression ($4\pi\eta a^3/3kT$) differ from the experimental values by a factor of about 15. The correlation time of translational motion is about 3 times that of rotational motion and it appears that the molecule reorientates substantially while moving by a distance of the order of one molecular diameter.

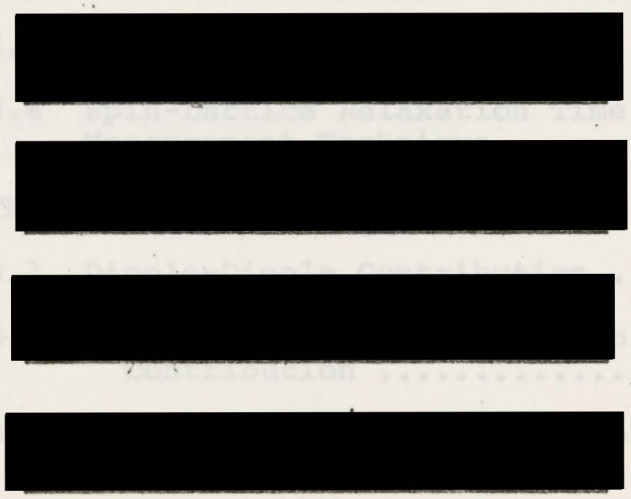

TABLE OF CONTENTS

LIST OF TABLES

LIST OF FIGURES

page

ACKNOWLEDGEMENTS

I would like to express my appreciation to Dr. H.S. Sandhu for his guidance and assistance throughout this work.

I am indebted to Dr. G.B. Friedman for his critical reading of the manuscript and suggestions. I would like to thank E.E. Ackroyd and J. Summers for many helpful suggestions in constructing the electronic apparatus.

The help given by A. Eisenberg with the glass-work on the vacuum system is greatly appreciated. I wish to thank my wife, Terry, for her patience and care in typing this thesis.

The financial assistance received from the National Research Council of Canada and the University of Victoria through grants to my supervisor is gratefully acknowledged.

CHAPTER 1

INTRODUCTION

In 1946 the nuclear magnetic resonance (NMR) phenomenon was observed in bulk matter for the first time, independently by Purcell et al. (1946) and Bloch et al. (1946). Since this breakthrough NMR has been used as a tool in the investigation of a variety of topics, e.g. the determination of chemical shifts, the determination of magnetic moments, the identification of nuclei present in a given substance and the study of microdynamic behaviour of molecules in matter.

A simple picture of what is meant by magnetic resonance is as follows: Many nuclei possess a magnetic moment $\bar{\mu}$ and an intrinsic spin or angular momentum $\bar{I}\hbar$. When a free nuclear spin is placed in a steady magnetic field $\bar{H}_0$ as shown in Fig. 1, the magnetic moment vector will precess about $\bar{H}_0$. The frequency of precession ω_0 is determined by the Larmor relation $\omega_0 = \gamma H_0$ where γ is the gyromagnetic ratio of the spin. If one now applies a field $\bar{H}_1$ normal to $\bar{H}_0$ and rotating at some angular frequency ω about $\bar{H}_0$, a torque will be exerted on $\bar{\mu}$ causing the angle θ between $\bar{H}_0$ and $\bar{\mu}$ to change. If $\omega \neq \omega_0$ or the sense of rotation of $\bar{H}_1$ is opposite to that of $\bar{\mu}$ then the phase between

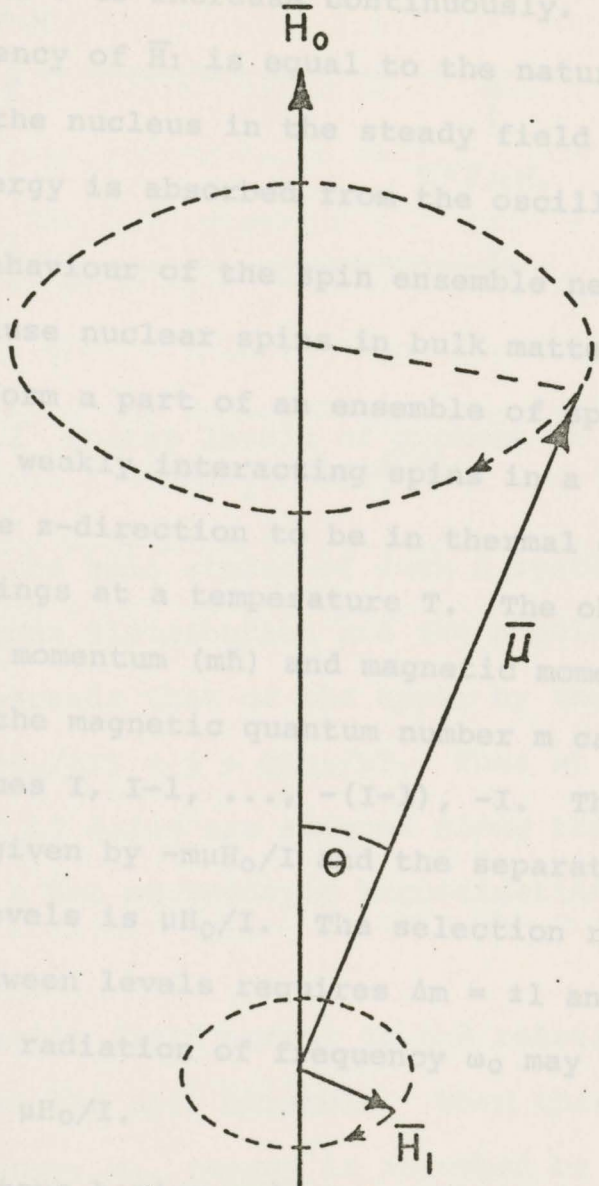

Fig. 1 Larmor precession of $\bar{\mu}$ about the magnetic field $\bar{H}_0$

$\overline{H_1}$ and $\overline{\mu}$ will be continuously changing with time and the torque will produce no net effect. If $\overline{H_1}$ is made to rotate in synchronism with $\overline{\mu}$ at the frequency ω_0, the torque will cause the angle θ to increase continuously. Thus when the angular frequency of $\overline{H_1}$ is equal to the natural precessional frequency of the nucleus in the steady field $\overline{H_0}$, resonance occurs and energy is absorbed from the oscillating field $\overline{H_1}$.

The behaviour of the spin ensemble needs now to be described because nuclear spins in bulk matter are not isolated but form a part of an ensemble of spins. Consider an ensemble of weakly interacting spins in a steady magnetic field $\overline{H_0}$ in the z-direction to be in thermal equilibrium with their surroundings at a temperature T. The observable values of the angular momentum ($m\hbar$) and magnetic moment ($m\mu/I$) are quantized and the magnetic quantum number m can take any of the (2I+1) values I, I-1, ..., -(I-1), -I. The energy of each level is given by $-m\mu H_0/I$ and the separation between the adjacent levels is $\mu H_0/I$. The selection rule for transitions between levels requires $\Delta m = \pm 1$ and thus electromagnetic radiation of frequency ω_0 may cause transitions for $\hbar\omega_0 = \mu H_0/I$.

For protons having spin I = 1/2, there are only two energy levels corresponding to the spins being parallel or

anti-parallel to $\bar{H}_0$ as shown in Fig. 2. At thermal

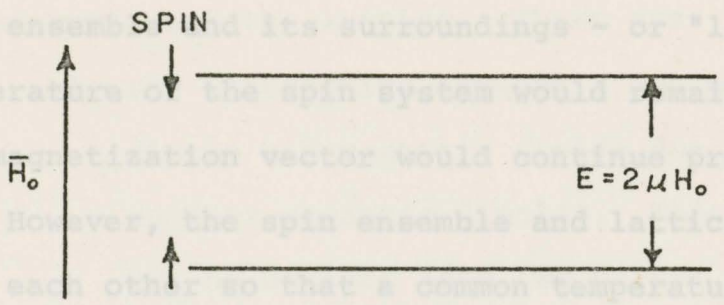

Fig. 2 Energy levels of protons in a magnetic field. $\bar{H}_0$

equilibrium, the spin states of such a system are governed by the Boltzmann distribution and the population of the lower state exceeds that of the upper by the Boltzmann factor $\exp(2\mu H_0/kT) \simeq 1 + 2\mu H_0/kT$. Thus at equilibrium a larger number of spins are aligned along the direction of $\bar{H}_0$ producing a net macroscopic magnetization $\bar{M}_0$ in the z-direction.

A magnetic field normal to and rotating about $\bar{H}_0$ is now applied to the spin ensemble. When this field is of the Larmor frequency, ω_0, energy is absorbed by the ensemble. This results in an increase in the temperature of the spin ensemble and an increase in the number of spins in the upper state, thereby causing a change in the z-component of the magnetization $\bar{M}$. The magnetization vector will now precess

about $\bar{H}_0$ and will have the z-component M_z smaller in magnitude than the equilibrium value $\bar{M}_0$. The rotating field is now removed. If no coupling existed between the spin ensemble and its surroundings - or "lattice" - the temperature of the spin system would remain unchanged and the magnetization vector would continue precessing about $\bar{H}_0$. However, the spin ensemble and lattice are in "contact" with each other so that a common temperature will again be reached and M_z will attain its equilibrium value $\bar{M}_0$. Bloch (1946) considered the return of M_z towards $\bar{M}_0$ to be exponential with a characteristic time constant T_1 which is known as the spin-lattice relaxation time. The rate of change of M_z is given by the following differential equation (Bloch 1946)

$$\frac{dM_z(t)}{dt} = -\frac{M_z(t) - M_0}{T_1} \qquad (1.1)$$

If the initial value of $M_z=0$ at $t=0$, the solution of eq.(1.1) becomes

$$M_z(t) = M_0\left[1 - \exp(-t/T_1)\right] \qquad (1.2)$$

Thus for $t=T_1$, the z-component of $\bar{M}$ equals 0.632 $\bar{M}_0$. In other words T_1 is the time taken for M_z to recover to 63.2% of its equilibrium value $\bar{M}_0$.

Once the spin ensemble has been perturbed, it will

return to thermal equilibrium - or relax - by interacting with the lattice. Different relaxation mechanisms may contribute in establishing thermal equilibrium between the spin ensemble and the lattice. These are:

a) the interaction between a nuclear magnetic dipole and magnetic fields due to other nuclear magnetic dipoles. This interaction can be divided into two parts:
   1) the intramolecular dipole-dipole interaction between nuclei on the same molecule. The contribution to this interaction arises from the rotational or tumbling motion of molecules.
   2) the intermolecular dipole-dipole interaction between nuclei on different molecules which results from the translational motion of molecules.

b) the interaction between the nuclear magnetic dipole and the magnetic fields due to electric currents which are produced by the charges of a rotating molecule - the spin-rotational interaction.

c) the interaction between the electric quadrupole moment of a nucleus and the electric field gradient at the nucleus due to surrounding

electrons and nuclei. Only nuclei with spin $I \geq 1$ possess a quadrupole moment and thus this interaction need not be considered for nuclei with $I < 1$.

It is of interest to obtain information about the different relaxation mechanisms occurring in a given substance in order to gain some understanding about molecular motion. Each of the relaxation mechanisms a, b and c can contribute to the relaxation. T_1 obtained from experiment is a measure of the total contribution arising from the various relaxation mechanisms and cannot give the separate contributions directly. However the intermolecular dipole-dipole contribution can be separated from the other contributions (intramolecular dipole-dipole and spin-rotational contributions) by studying T_1 in a given liquid as a function of concentration in certain other liquids (CS_2, CCl_4 or the perdeuterated analog of the liquid). The intramolecular dipole-dipole and spin-rotational contributions can then be separated by studying T_1 of deuterons in the perdeuterated analog of the given liquid.

This thesis deals with the separation of the various mechanisms contributing to relaxation in liquid methylene iodide (CH_2I_2) in order to gain some information about molecular motions in this liquid.

Measurements of deuteron T_1 in oxygen-free samples of CD_2I_2 and proton T_1 in oxygen-free samples of 100% CH_2I_2, 80% CH_2I_2 - 20% CD_2I_2, 60% CH_2I_2 - 40% CD_2I_2 and 40% CH_2I_2 - 60% CD_2I_2 by volume have been carried out between 7°C to 100°C. The different contributions have been separated and it is found that the intramolecular dipole-dipole contribution amounts to 67.5% of the total relaxation while the intermolecular dipole-dipole contribution amounts to about 32.5% of the total relaxation over the temperature range studied. Results indicate that spin-rotation interaction makes no contribution in the temperature range studied.

In Chapter 2 the experimental apparatus and the experimental technique for spin-lattice relaxation time measurements are described. Chapter 3 deals with the theory of spin-lattice relaxation. The experimental results are presented and discussed in Chapter 4. In Chapter 5 the results are summarized and the conclusions reached from this work given.

CHAPTER 2

EXPERIMENTAL APPARATUS AND RELAXATION TIME MEASUREMENT TECHNIQUE

2.1 The Spectrometer

The basic arrangement of the 4 Mc/sec spectrometer is shown in Fig. 3. It is similar to that described by Hahn (1950) and is simple and straightforward. A brief discussion of the equipment follows.

2.1.1 DC Magnet

The magnet used in this work was a Magnion Model L-75 Laboratory Electromagnet having 17.8 cm (or 7") diameter pole faces. The magnet is capable of supplying fields up to 7000 gauss with an air gap of 5.7 cm.

2.1.2 Pulse Generating System

Two Tektronix Type 162 Waveform Generators (A and B) and three Tektronix Type 163 Pulse Generators (C, D and E) were connected as shown in Fig. 4 to produce two equal pulses of adjustable width, amplitude and pulse interval.

The time base for the pulse generating system was derived from generator A which was set in the recurrent mode of operation and produced rectangular pulses at variable repetition frequency. The output pulses from generators C and D could be positioned anywhere in time between the

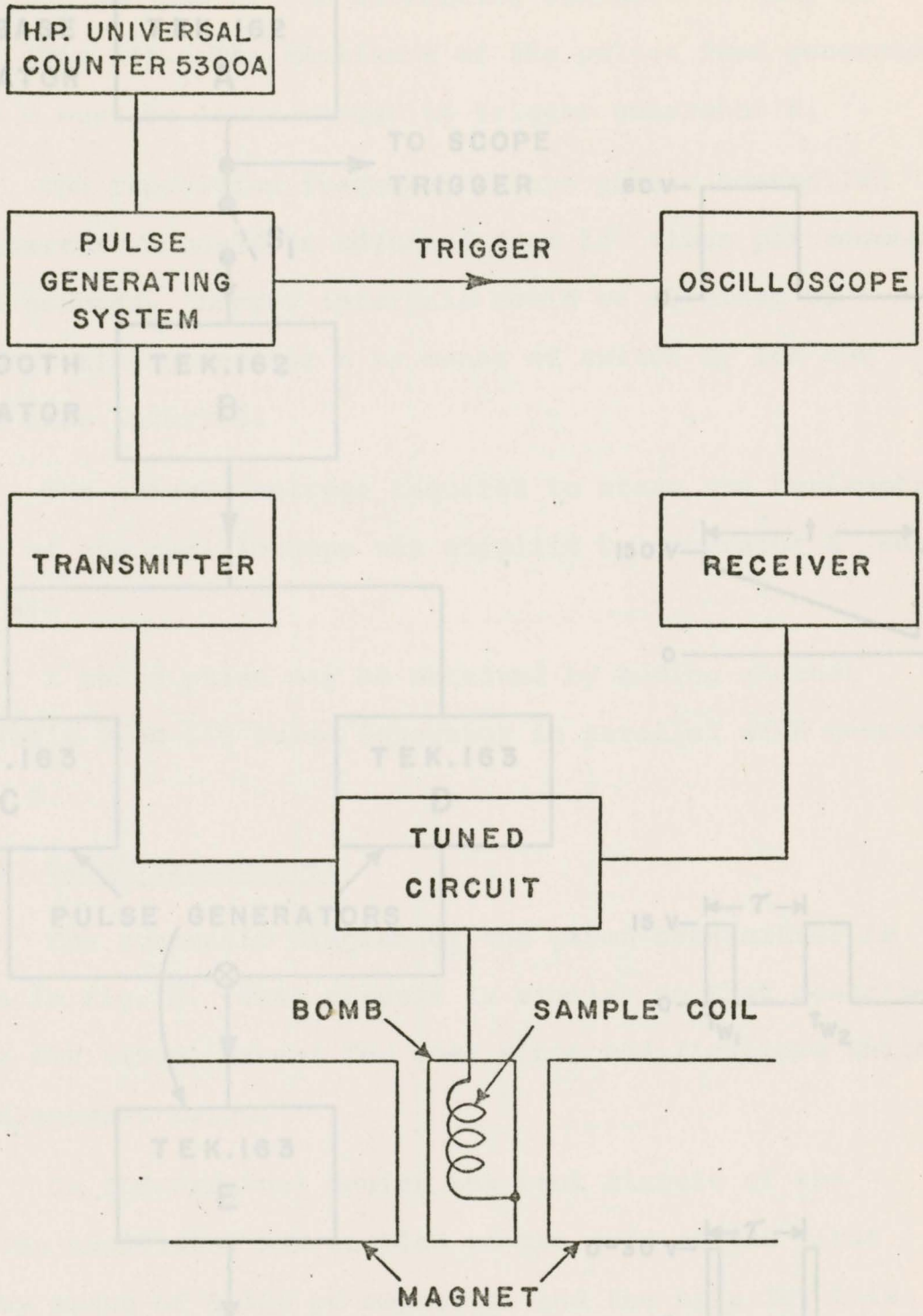

Fig. 3 Block diagram of the 4 Mc/sec NMR Spectrometer

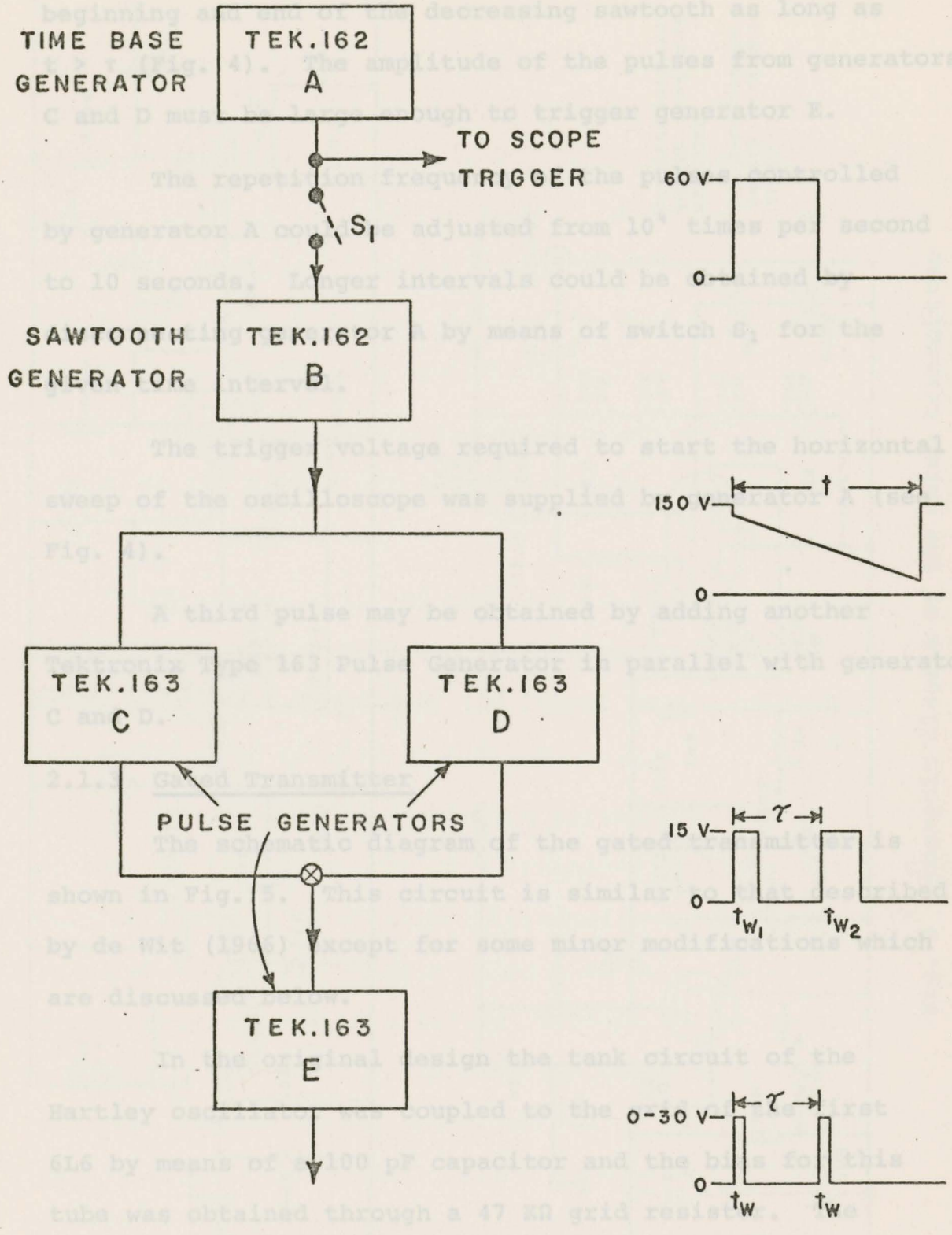

Fig. 4 Pulse generating system

beginning and end of the decreasing sawtooth as long as $t > \tau$ (Fig. 4). The amplitude of the pulses from generators C and D must be large enough to trigger generator E.

The repetition frequency of the pulses controlled by generator A could be adjusted from 10^4 times per second to 10 seconds. Longer intervals could be obtained by disconnecting generator A by means of switch S_1 for the given time interval.

The trigger voltage required to start the horizontal sweep of the oscilloscope was supplied by generator A (see Fig. 4).

A third pulse may be obtained by adding another Tektronix Type 163 Pulse Generator in parallel with generators C and D.

2.1.3 Gated Transmitter

The schematic diagram of the gated transmitter is shown in Fig. 5. This circuit is similar to that described by de Wit (1966) except for some minor modifications which are discussed below.

In the original design the tank circuit of the Hartley oscillator was coupled to the grid of the first 6L6 by means of a 100 pF capacitor and the bias for this tube was obtained through a 47 KΩ grid resistor. The cathode of the first 6L6 was connected directly to the

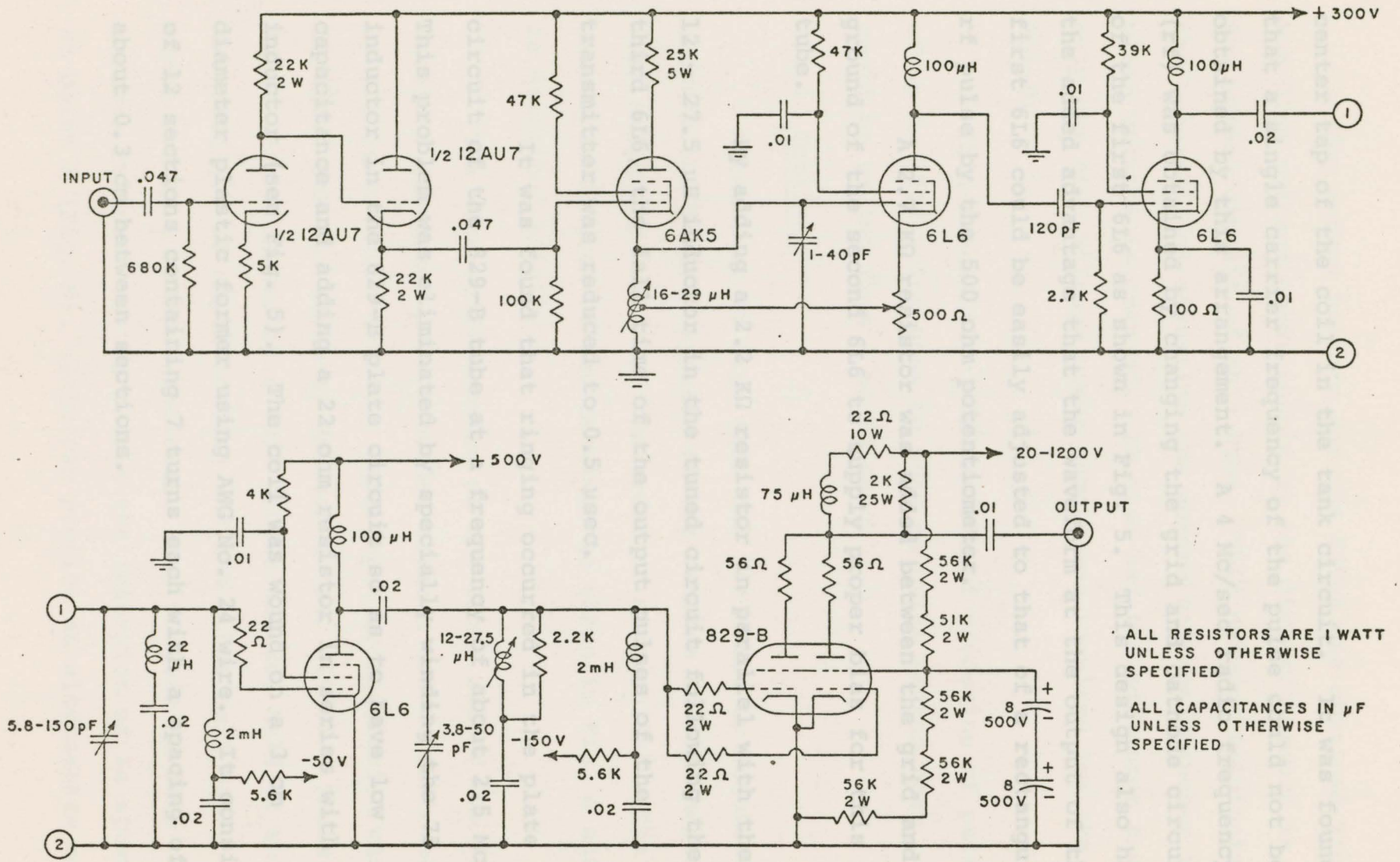

Fig. 5 Schematic diagram of the gated transmitter

center tap of the coil in the tank circuit. It was found that a single carrier frequency of the pulse could not be obtained by this arrangement. A 4 Mc/sec radio frequency (rf) was obtained by changing the grid and cathode circuit of the first 6L6 as shown in Fig. 5. This design also had the added advantage that the waveform at the output of the first 6L6 could be easily adjusted to that of a rectangular rf pulse by the 500 ohm potentiometer.

A 2.7 KΩ resistor was added between the grid and ground of the second 6L6 to supply proper bias for this tube.

By adding a 2.2 KΩ resistor in parallel with the 12 - 27.5 μH inductor in the tuned circuit following the third 6L6, the fall time of the output pulses of the transmitter was reduced to 0.5 μsec.

It was found that ringing occurred in the plate circuit of the 829-B tube at a frequency of about 2.5 Mc/sec. This problem was eliminated by specially winding the 75 μH inductor in the 829-B plate circuit so as to have low capacitance and adding a 22 ohm resistor in series with the inductor (see Fig. 5). The coil was wound on a 3 cm diameter plastic former using AWG No. 24 wire. It consisted of 12 sections containing 7 turns each with a spacing of about 0.3 cm between sections.

The screen voltage for the 829-B was obtained from the high voltage power supply by the divider network in the screen circuit of this tube. This network eliminated the necessity of adjusting the screen voltage whenever the plate voltage is changed. It also had the advantage that only one high voltage power supply was required for the 829-B.

This transmitter was capable of producing rf pulses of up to 1500 volts peak to peak at pulse widths that could be varied from 2 to 60 μsec.

2.1.4 Receiver

A receiver of high gain and low noise is required because the nuclear signals of the samples studied here were extremely small (of the order of microvolts). The schematic diagram of the receiver is shown in Fig. 6 and is described briefly.

The tube configuration of the front end of the receiver consisted of a grounded-cathode triode followed by a grounded-grid triode. This input configuration was designed for low noise by Wallman et al. (1948). These tubes were followed by a 6DJ8 double triode, half of which was used for rf amplification and the other half was connected as a cathode follower. The purpose of this cathode follower was to permit the insertion of an attenuator at point A (Fig. 6). This can provide an alternative method

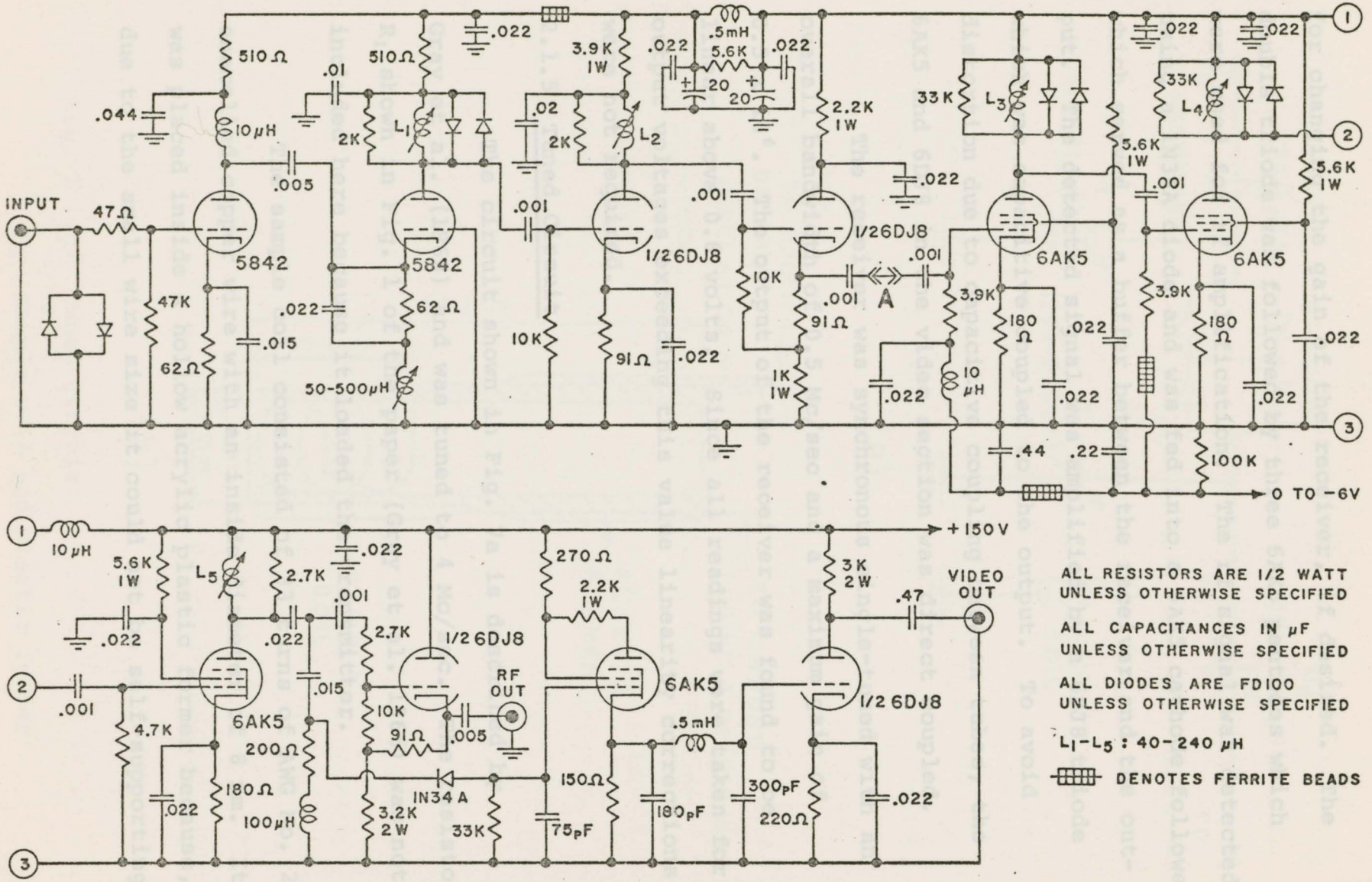

Fig. 6 Schematic diagram of the receiver

for changing the gain of the receiver, if desired. The double triode was followed by three 6AK5 pentodes which were used for rf amplification. The rf signal was detected using a 1N34A diode and was fed into a 6AK5 cathode follower which served as a buffer between the receiver and the output. The detected signal was amplified by a 6DJ8 triode which was capacitive coupled to the output. To avoid distortion due to capacitive coupling between tubes, the 6AK5 and 6DJ8 in the video section was direct coupled.

The receiver was synchronous single-tuned with an overall bandwidth of 0.5 Mc/sec and a maximum gain of 0.5×10^6. The output of the receiver was found to be linear above 0.6 volts. Since all readings were taken for output voltages exceeding this value linearity corrections were not required.

2.1.5 Tuned Circuit

The circuit shown in Fig. 7a is described by Gray et al. (1966) and was tuned to 4 Mc/sec. The resistor R_1 shown in Fig. 1 of the paper (Gray et al. 1966) was not included here because it loaded the transmitter.

The sample coil consisted of 33 turns of AWG No. 26 enamelled copper wire with an inside diameter of 8 mm. It was placed inside a hollow acrylic plastic former because, due to the small wire size it could not be self-supporting.

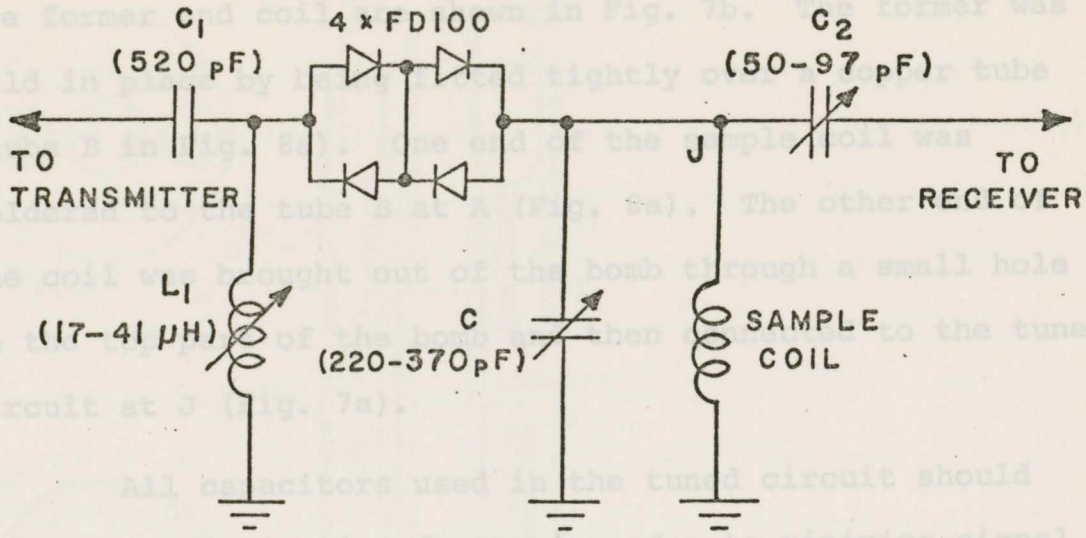

(a)

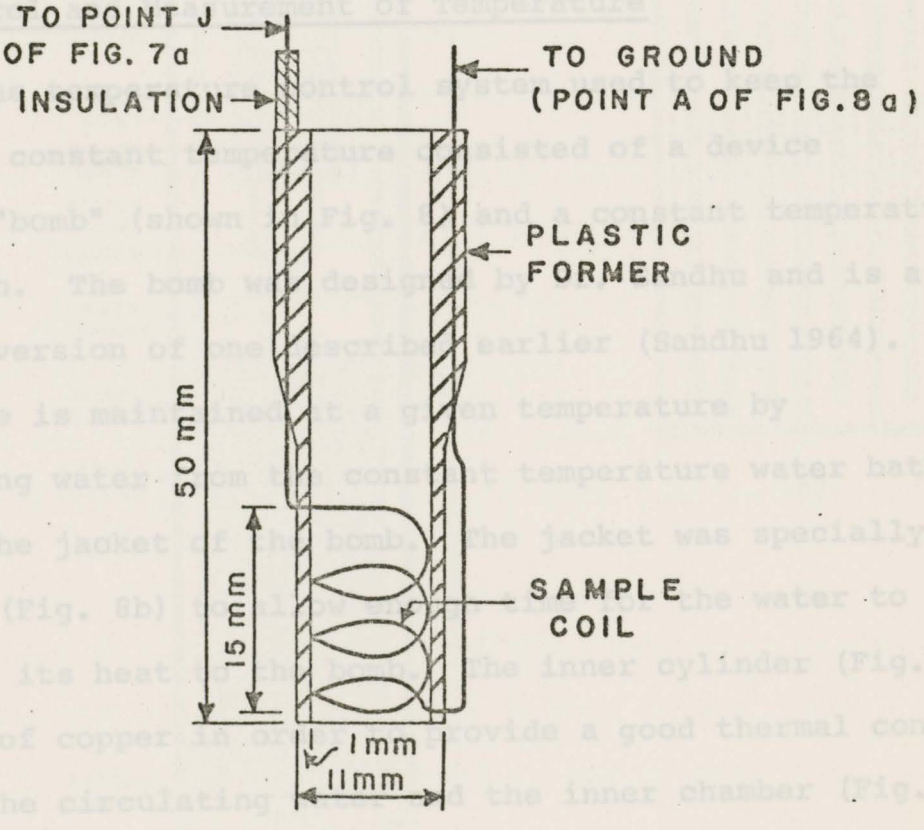

(b)

Fig. 7 (a) Tuned circuit

(b) Sample coil and plastic former

The former and coil are shown in Fig. 7b. The former was held in place by being fitted tightly over a copper tube (tube B in Fig. 8a). One end of the sample coil was soldered to the tube B at A (Fig. 8a). The other end of the coil was brought out of the bomb through a small hole in the top part of the bomb and then connected to the tuned circuit at J (Fig. 7a).

All capacitors used in the tuned circuit should have a low dissipation factor in order to minimize signal loss.

2.2 Control and Measurement of Temperature

The temperature control system used to keep the sample at constant temperature consisted of a device called a "bomb" (shown in Fig. 8) and a constant temperature water bath. The bomb was designed by Dr. Sandhu and is a modified version of one described earlier (Sandhu 1964). The sample is maintained at a given temperature by circulating water from the constant temperature water bath through the jacket of the bomb. The jacket was specially designed (Fig. 8b) to allow enough time for the water to dissipate its heat to the bomb. The inner cylinder (Fig. 8a) was made of copper in order to provide a good thermal contact between the circulating water and the inner chamber (Fig. 8a)

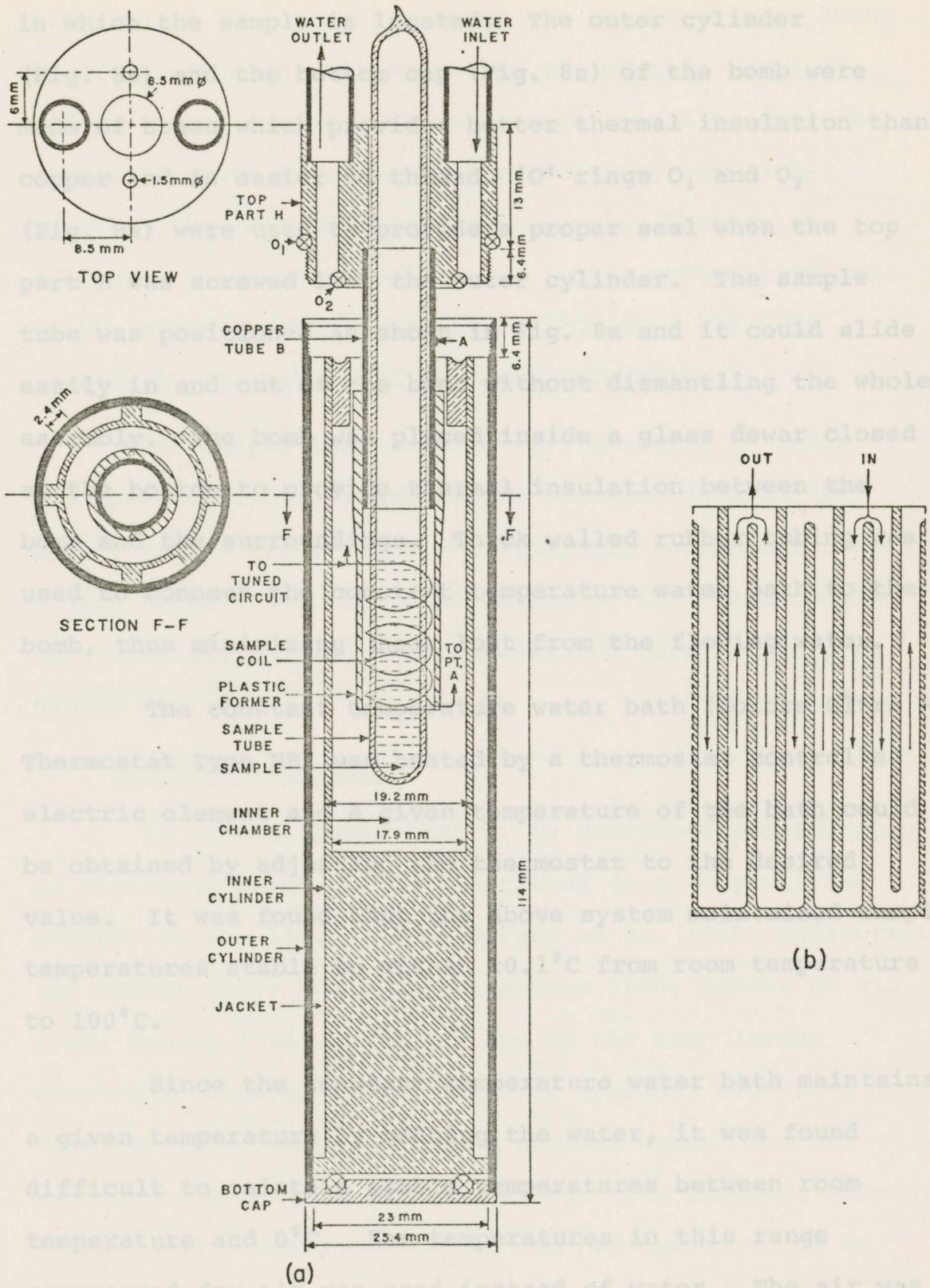

Fig. 8 (a) Bomb
(b) Specially designed jacket machined on outside of inner copper cylinder

in which the sample is located. The outer cylinder (Fig. 8a) and the bottom cap (Fig. 8a) of the bomb were made of brass which provides better thermal insulation than copper and is easier to thread. 'O' rings O_1 and O_2 (Fig. 8a) were used to provide a proper seal when the top part H was screwed into the outer cylinder. The sample tube was positioned as shown in Fig. 8a and it could slide easily in and out of the bomb without dismantling the whole assembly. The bomb was placed inside a glass dewar closed at the bottom to provide thermal insulation between the bomb and the surroundings. Thick walled rubber tubing was used to connect the constant temperature water bath to the bomb, thus minimizing heat lost from the flowing water.

The constant temperature water bath (Colora Ultra - Thermostat Type NB) was heated by a thermostat controlled electric element and a given temperature of the bath could be obtained by adjusting the thermostat to the desired value. It was found that the above system maintained sample temperatures stable to within $\pm 0.1^{\circ}C$ from room temperature to $100^{\circ}C$.

Since the constant temperature water bath maintains a given temperature by heating the water, it was found difficult to maintain stable temperatures between room temperature and $0^{\circ}C$. For temperatures in this range compressed dry air was used instead of water. The air was cooled by passing it through a coil of copper tubing

immersed in an ice-salt mixture. A two layer coil about 15 cm in diameter and consisting of about 60 turns of 0.6 cm copper tubing provided enough length to cool the sample to about $0^{\circ}C$. The temperature was varied by changing the rate of flow of air passing through the system by means of a needlevalve. This system provided stable temperatures to within $\pm 0.1^{\circ}C$ for 1 - 2 hour periods in the range $0^{\circ}C$ to room temperature.

The sample temperatures were measured by means of a copper-constantan thermocouple soldered at A to the copper tube B (Fig. 8a) and a Honeywell Portable Potentiometer Model 2746. The calibration of the thermocouple was carefully checked and temperatures were measured to within $\pm 0.1^{\circ}C$.

2.3 Sample Purification

It is well known that T_1 is decreased considerably if dissolved paramagnetic impurities (e.g. oxygen) are present in the liquid (Bloembergen et al. 1948; Nederbragt and Reilly 1956; Nolle and Mahendroo 1960; Sandhu et al. 1960; Sandhu 1966). This is due to the much larger electronic moments of paramagnetic species, resulting in a larger interaction between a nuclear moment and the electronic moment of such a species. The samples, obtained commercially, contained oxygen and had therefore to be purified.

There are several techniques available for obtaining oxygen-free samples and two commonly used techniques are:

1) the gettering technique (Nolle and Mahendroo 1960; Sandhu et al. 1960; Lees et al. 1961; Sandhu 1971a)

2) the freeze-pump-thaw technique (Nederbragt and Reilly 1956; Nolle and Mahendroo 1960; Sandhu 1969).

Although both techniques are equally effective in removing oxygen, the samples were purified using the freeze-pump-thaw technique because it is somewhat simpler to use than the gettering technique. In brief the purification technique was as follows:

The schematic diagram of the purification system is shown in Fig. 9. Three Pyrex glass traps M_1, M_2 and M_3 were connected to copper tubing of about 3 cm in diameter. All metal valves V_1 - V_6 are greasefree so as to prevent contamination of the sample. In a typical sample purification, the system was pumped to a pressure of about 10^{-6} mm of mercury and baked several times during pumping in order to remove oxygen molecules adsorbed on the walls. The Pyrex glass tube G was thoroughly cleaned and boiled in distilled water for approximately 3/4 of an hour. It was then dried with hot air. The tube G, filled with about

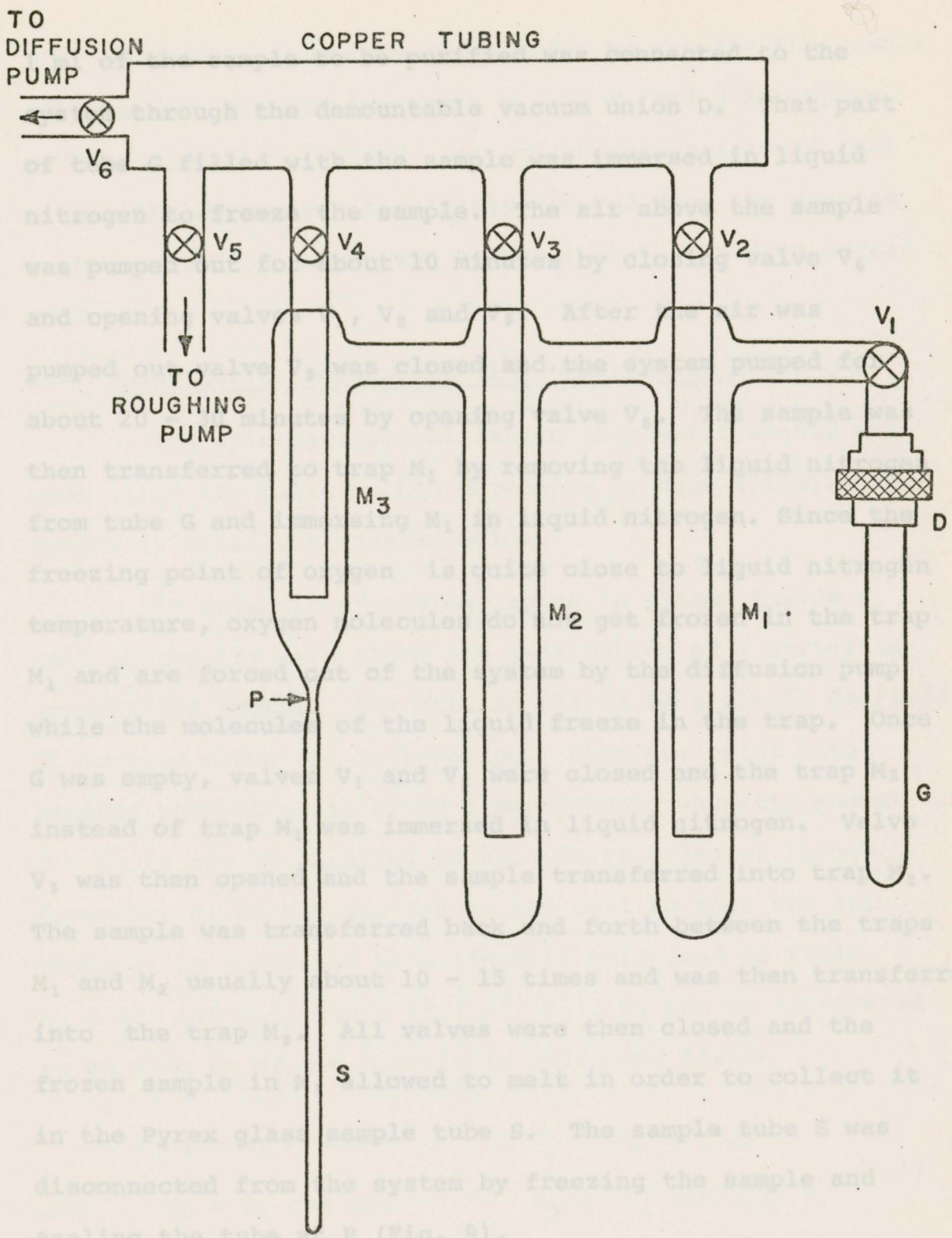

Fig. 9 Schematic diagram of purification system

1 ml of the sample to be purified was connected to the system through the demountable vacuum union D. That part of tube G filled with the sample was immersed in liquid nitrogen to freeze the sample. The air above the sample was pumped out for about 10 minutes by closing valve V_6 and opening valves V_1, V_2 and V_5. After the air was pumped out valve V_5 was closed and the system pumped for about 20 - 30 minutes by opening valve V_6. The sample was then transferred to trap M_1 by removing the liquid nitrogen from tube G and immersing M_1 in liquid nitrogen. Since the freezing point of oxygen is quite close to liquid nitrogen temperature, oxygen molecules do not get frozen in the trap M_1 and are forced out of the system by the diffusion pump while the molecules of the liquid freeze in the trap. Once G was empty, valves V_1 and V_2 were closed and the trap M_2 instead of trap M_1 was immersed in liquid nitrogen. Valve V_3 was then opened and the sample transferred into trap M_2. The sample was transferred back and forth between the traps M_1 and M_2 usually about 10 - 15 times and was then transferred into the trap M_3. All valves were then closed and the frozen sample in M_3 allowed to melt in order to collect it in the Pyrex glass sample tube S. The sample tube S was disconnected from the system by freezing the sample and sealing the tube at P (Fig. 9).

fields given by eq.(2.1) will be in phase with the precession of $\bar{M}$ and will tip the magnetic moment vector away from the direction of $\bar{H}_0$ by an angle

$$\theta = \gamma H_1 t_w \qquad (2.2)$$

where t_w is the width of the rf pulse. The other circularly polarized field is out of phase with the precession of $\bar{M}$ and has no appreciable effect (Bloch and Siegert 1940).

The magnetic moment vector $\bar{M}$, precessing about $\bar{H}_0$ at an angle θ, will have a component in the x-y plane rotating about $\bar{H}_0$ and as a result an rf voltage is induced into the same coil used for the generation of the rf field. This induced voltage will be maximum when the magnetic moment vector $\bar{M}$ is in the x-y plane, i.e. when $\theta = \pi/2$. The induced voltage decays due to damping effects such as spin-lattice relaxation, spin-spin relaxation, an inhomogeneous dc field, etc. Thus a decaying signal called an induction tail is observed following the rf pulse.

If a second pulse is applied at a time $\tau < T_1$ after the first pulse, an induction tail is also observed after the second pulse. The maximum amplitude of this induction tail depends upon the regrowth of the z-component of the magnetization. The induction tails observed following a pair of equal pulses applied to a spin ensemble initially

at thermal equilibrium are shown in Fig. 10. A(0) and

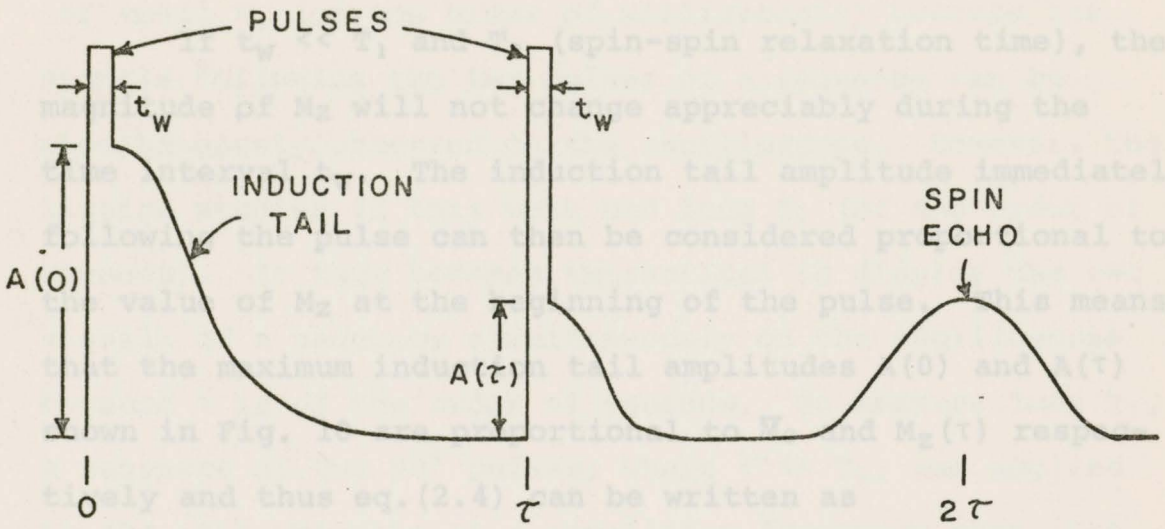

Fig. 10 NMR signal resulting from two equal pulses

$A(\tau)$ are the maximum induction tail amplitudes following the first and second pulse respectively. The signal at 2τ is due to constructive interference between precessing magnetic moments, and Hahn (1950), who first observed this signal has called it a "spin echo".

If a pulse of width t_w is applied to a spin ensemble at time $t = 0$, then immediately following the pulse $t = t_w$ and M_z (z-component of $\bar{M}$) is equal to $M_z(t_w)$. Solving eq.(1.1) using these initial conditions leads to

$$M_z(t) - M_0 = \left[M_z(t_w) - M_0\right] \exp\left[-(t-t_w)/T_1\right] \quad . \quad (2.3)$$

For $t = \tau$ and $t_w \ll \tau$, eq.(2.3) becomes

$$M_o - M_z(\tau) = \text{Constant} \exp(-\tau/T_1) \quad . \qquad (2.4)$$

If $t_w \ll T_1$ and T_2 (spin-spin relaxation time), the magnitude of M_z will not change appreciably during the time interval t_w. The induction tail amplitude immediately following the pulse can then be considered proportional to the value of M_z at the beginning of the pulse. This means that the maximum induction tail amplitudes $A(0)$ and $A(\tau)$ shown in Fig. 10 are proportional to $\overline{M}_o$ and $M_z(\tau)$ respectively and thus eq.(2.4) can be written as

$$A(0) - A(\tau) = \text{Constant} \exp(-\tau/T_1) \quad . \qquad (2.5)$$

Method I -

In practice, T_1 may be measured by applying two 90^0 ($\theta = \pi/2$) pulses separated by a time interval τ. The first 90^0 pulse perturbs the spin ensemble, which is initially at thermal equilibrium, and the second 90^0 pulse gives an indication of the extent M_z has recovered towards its equilibrium value in the time τ. The sequence of two 90^0 pulses is repeated for different values of τ at a repetition frequency that allows enough time between successive sequences for the spin ensemble to reach thermal equilibrium. Measuring the amplitude $A(\tau)$ as a function of τ, T_1 is found from the slope of a plot of $\ln\left[A(0) - A(\tau)\right]$ against τ.

Method II -

The method described above can be conveniently used for small T_1 (of the order of milliseconds) because the signals following the two pulses of a sequence can be simultaneously observed on the oscilloscope. However, the liquids studied in this work had long T_1 (of the order of seconds). It thus becomes impractical to display the two signals of a sequence simultaneously on the oscilloscope because τ is of the order of seconds. To measure long T_1, a sequence of two 90^0 pulses, where $\tau << T_1$, was applied to the spin ensemble at a repetition frequency such that the times t between successive sequences was of the order of T_1. The maximum amplitude of the induction tail following the first 90^0 pulse of a sequence is proportional to the value of $M_z(t)$ at the beginning of the sequence and is denoted by A(t). In order to obtain a value of A(t) proportional to $\bar{M}_0$ the system was given sufficient time to reach thermal equilibrium (about $10T_1$) and then a sequence of 90^0 pulses was applied. The maximum amplitude of the induction tail following the first pulse in this sequence is denoted by $A(\infty)$. T_1 was measured by applying sequences of pulses at different repetition frequencies, thus obtaining values of A(t) as a function of t. Replacing A(0) by $A(\infty)$ and $A(\tau)$ by A(t) eq.(2.5) becomes

$$A(\infty) - A(t) = \text{Constant} \exp(-t/T_1) \qquad (2.6)$$

and T_1 was obtained from the slope of a plot of $\ln\left[A(\infty) - A(t)\right]$ against t.

The induction tails were observed with a Tektronix Type 555 Oscilloscope and the amplitudes of the signals were measured directly from the oscilloscope.

CHAPTER 3

THEORY OF SPIN-LATTICE RELAXATION

In liquids molecules are constantly moving due to thermal agitation. The motion of the molecules is random Brownian motion. As a result of this motion nuclei are subjected to rapidly fluctuating magnetic and electric fields due to neighboring molecular nuclei and electrons. These random fluctuations comprise a spectrum of frequencies. If some of these frequencies satisfy the resonance condition of a given nucleus, transitions between the energy levels of the nucleus may result. The relaxation rate, $1/T_1$ is directly proportional to the probability of such transitions and is given by

$$(1/T_1)_{total} = (1/T_1)_{dd} + (1/T_1)_{sr} + (1/T_1)_{q} \qquad (3.1)$$

where $(1/T_1)_{dd}$ is the contribution arising from dipole-dipole interaction,

$(1/T_1)_{sr}$ is the contribution due to spin-rotation interaction,

$(1/T_1)_{q}$ is the contribution resulting from quadrupolar interaction.

These contributions are discussed in turn in the following three sections.

3.1 Dipole-Dipole Contribution

Consider a spin I_j interacting with spin I_k. Such an ensemble of spins located in a steady field $\bar{H}_o$ may be described by the following Hamiltonian

$$\mathcal{H} = \mathcal{H}_o + \mathcal{H}'(t) \tag{3.2}$$

where $\mathcal{H}_o$ is the unperturbed Hamiltonian giving the Zeeman energies $-\bar{\mu}\cdot\bar{H}_o$ and $\mathcal{H}'(t)$ is a random perturbation term describing the magnetic interaction due to fluctuating fields. For nucleus j one may write

$$\mathcal{H}'_j(t) = \sum_k \mathcal{H}_{jk}(t) \tag{3.3}$$

where $\mathcal{H}_{jk}(t)$ represents the dipole-dipole interaction between the spins I_j and I_k. The relaxation rate corresponding to dipolar interactions may be found by determining the probability of transitions induced by $\mathcal{H}'_j(t)$.

Consider the two spins I_j and I_k joined by the vector $\bar{r}_{jk}$ whose polar and azimuthal angles are θ_{jk} and ϕ_{jk} respectively. In this case the perturbing Hamiltonian $\mathcal{H}_{jk}(t)$ is commonly written as (Bloembergen et al. 1948)

$$\mathcal{H}_{jk}(t) = \gamma_j\gamma_k\hbar^2(A + B + C + D + E + F) \tag{3.4a}$$

where
$$A = I_{zj} I_{zk} F^0_{jk}$$
$$B = -(1/4)(I^+_j I^-_k + I^-_j I^+_k) F^0_{jk}$$
$$C = -(3/2)(I^+_j I_{zk} + I_{zj} I^+_k) F^1_{jk}$$
$$D = C^* = -(3/2)(I^-_j I_{zk} + I_{zj} I^-_k) F^{1*}_{jk}$$
$$E = -(3/4) I^+_j I^+_k F^2_{jk}$$
$$F = E^* = -(3/4) I^-_j I^-_k F^{2*}_{jk} \qquad (3.4b)$$

and
$$F^0_{jk} = r^{-3}_{jk}\left[1 - 3\cos^2\theta_{jk}(t)\right]$$
$$F^1_{jk} = r^{-3}_{jk}\sin\theta_{jk}(t)\cos\theta_{jk}(t)\exp\left[-i\phi_{jk}(t)\right] \qquad (3.4c)$$
$$F^2_{jk} = r^{-3}_{jk}\sin^2\theta_{jk}(t)\exp\left[-2i\phi_{jk}(t)\right]$$

with * indicating the complex conjugate

$I^{\pm}$ are raising and lowering operators defined by $I^{\pm} = I_x \pm iI_y$.

The F_{jk}'s given in eq.(3.4c) are time dependent position functions and describe the spatial orientation of the fluctuating magnetic field produced by nucleus k at the site of nucleus j. The different terms of $\mathcal{H}_{jk}(t)$

induce certain types of transitions which may be found from the spin operators indicated in eq.(3.4b).

Let m, m_j and m_k be the total magnetic quantum number, the magnetic quantum number for the jth nucleus and the magnetic quantum number for the kth nucleus respectively. For terms A and B of eq.(3.4a), $\Delta m = 0$ because for term A m_j and m_k remain unchanged and for term B either $\Delta m_j = +1$ and $\Delta m_k = -1$ or $\Delta m_j = -1$ and $\Delta m_k = +1$. Therefore term A and B do not cause energy changes of the spin ensemble. Term C induces transitions for which $\Delta m_j = +1$ or $\Delta m_k = +1$ and thus $\Delta m = +1$. For term D $\Delta m_j = -1$ or $\Delta m_k = -1$ and therefore $\Delta m = -1$. Term E involves the raising of m_j and m_k resulting in $\Delta m = +2$ while for term F $\Delta m_j = \Delta m_k = -1$ and thus $\Delta m = -2$. Thus, terms C, D, E and F produce exchanges of energy between the spin ensemble and the lattice.

The probability of the transitions of $\mathcal{H}_{jk}(t)$ brought about by term A can be evaluated from the following expression

$$P_a = (1/\hbar^2)\int_{-\infty}^{\infty} \langle \mathcal{H}^{A}_{jk}(t)\, \mathcal{H}^{A*}_{jk}(t+\tau)\rangle\, e^{i\omega\tau} d\tau \qquad (3.5)$$

where $\mathcal{H}^{A}_{jk}(t) = \gamma_j \gamma_k \hbar^2 A$

τ is a time interval

and $\langle\ \rangle$ indicates time averaging.

Similar expressions can be written for the transition probabilities due to the remaining terms of $\mathcal{H}_{jk}(t)$ by replacing $\mathcal{H}^{A}_{jk}$ in eq.(3.5) by the Hamiltonians $\mathcal{H}^{B}_{jk} = \gamma_j\gamma_k\hbar^2 B, \ldots, \mathcal{H}^{F}_{jk} = \gamma_j\gamma_k\hbar^2 F$. These transition probabilities depend on the degree of correlation between a position function at time t and its value at a later time $(t+\tau)$. As the position functions are fluctuating rapidly there is essentially no correlation for large enough values of τ. It is generally assumed that the behaviour of a position function with time can be expressed by a correlation function which decreases exponentially with τ as follows (Bloembergen et al. 1948)

$$G^{\alpha}(\tau) = \langle F^{\alpha}_{jk}(t) F^{\alpha *}_{jk}(t) \rangle e^{-|\tau|/\tau_c} \qquad (3.6)$$

where τ_c is called the correlation time and $\alpha = 0,1,2$. The Fourier transforms of $G^{\alpha}(\tau)$ are known as spectral densities and are defined by

$$J^{\alpha}(\omega) = \int_{-\infty}^{\infty} G^{\alpha}(\tau) e^{i\omega\tau} d\tau \ . \qquad (3.7)$$

These spectral densities can be evaluated by performing the integration in eq.(3.7) where the $G^{\alpha}(\tau)$'s have been replaced by eq.(3.6) and then time averaging the quantities $\langle F^{\alpha}_{jk}(t) F^{\alpha *}_{jk}(t) \rangle$. The resulting spectral densities are given by [Bloembergen et al. 1948, eqs.(43) and (45)]

$$J_0 = \frac{8 \langle r_{jk}^{-6} \rangle \tau_c}{5(1 + \omega^2 \tau_c^2)}$$

$$J_1 = \frac{4 \langle r_{jk}^{-6} \rangle \tau_c}{15(1 + \omega^2 \tau_c^2)} \qquad (3.8)$$

$$J_2 = \frac{16 \langle r_{jk}^{-6} \rangle \tau_c}{15(1 + \omega^2 \tau_c^2)} \quad .$$

In the theory of nuclear spin relaxation by Bloembergen et al. (1948), the relation between relaxation rates and the transition probabilities is obtained from rate equations that govern the populations of the different spin states. This theory assumes that the behaviour of a spin ensemble can be completely described through the populations of the ensemble's energy states. Such a description is in general incomplete (Abragam 1961, p. 26 and 275). A more general formulism has been developed by Wangsness and Bloch (1953), Kubo and Tomita (1954) and Redfield (1957) who describe the spin ensemble through a density matrix (Abragam 1961, p. 26). Evaluation of the relaxation rate due to dipolar spin-lattice interaction between identical spins ($I_j = I_k$) using the density matrix formulism yields the following

$$1/T_1 = (3/2) I(I+1) \gamma^4 \hbar^2 \left[J_1(\omega) + J_2(2\omega) \right] \quad . \qquad (3.9)$$

Substituting eq.(3.8) into eq.(3.9) gives the relaxation rate of a system of identical spins to be

$$(1/T_1)_{jj} = (2/5)I_j(I_j+1)\gamma_j^4\hbar^2 \sum_j \langle r_{jj}^{-6} \rangle \left[\frac{(\tau_c)_{jj}}{1 + \omega_j^2(\tau_c)_{jj}^2} + \frac{4(\tau_c)_{jj}}{1 + 4\omega_j^2(\tau_c)_{jj}^2} \right] \qquad (3.10)$$

where $(\tau_c)_{jj}$ is the correlation time involved in the reorientation of the internuclear vector $\bar{r}_{jj}$. Similarly the relaxation rate for the case of nonidentical spins ($I_j \neq I_k$) can be evaluated and is given by Blicharski et al. (1960) as

$$(1/T_1)_{jk} = (2/5)\gamma_j^2\hbar^2 \sum_k \gamma_k^2 I_k(I_k+1) \langle r_{jk}^{-6} \rangle \times \left[\frac{(1/3)(\tau_c)_{jk}}{1 + (\omega_j-\omega_k)^2(\tau_c)_{jk}^2} + \frac{(\tau_c)_{jk}}{1 + \omega_j^2(\tau_c)_{jk}^2} + \frac{2(\tau_c)_{jk}}{1 + (\omega_j+\omega_k)^2(\tau_c)_{jk}^2} \right] \qquad (3.11)$$

where $(\tau_c)_{jk}$ is the correlation time associated with the reorientation of the internuclear vector $\bar{r}_{jk}$. The total relaxation rate of spin j due to dipole-dipole interaction is equal to the sum of the contributions due to identical

spins and nonidentical spins. Combining eqs.(3.10) and (3.11) gives

$$(1/T_1)_{dd} = (2/5)\gamma_j^2\hbar^2 \left\{ \gamma_j^2 I_j(I_j+1) \sum_j \langle r_{jj}^{-6} \rangle \times \left[\frac{1}{1 + \omega_j^2(\tau_c)_{jj}^2} + \frac{4}{1 + 4\omega_j^2(\tau_c)_{jj}^2} \right] (\tau_c)_{jj} + \sum_k \gamma_k^2 I_k(I_k+1) \langle r_{jk}^{-6} \rangle \left[\frac{(1/3)}{1 + (\omega_j-\omega_k)^2(\tau_c)_{jk}^2} + \frac{1}{1 + \omega_j^2(\tau_c)_{jk}^2} + \frac{2}{1 + (\omega_j+\omega_k)^2(\tau_c)_{jk}^2} \right] (\tau_c)_{jk} \right\} . \quad (3.12)$$

Dipole-dipole interactions can be divided into parts:

1) intramolecular dipole-dipole interaction between nuclei on the same molecule whose contribution is represented by $(1/T_1)_{dd\text{-intra}}$,

2) intermolecular dipole-dipole interaction between nuclei located on different molecules or between nuclear spins and paramagnetic ions whose contribution is represented by $(1/T_1)_{dd\text{-inter}}$.

$(1/T_1)_{dd}$ is then written as

$$(1/T_1)_{dd} = (1/T_1)_{dd\text{-intra}} + (1/T_1)_{dd\text{-inter}} . \quad (3.13)$$

3.1.1 Intramolecular Dipole-Dipole Contribution

It is often assumed that the rotational motion of the molecule in a liquid is similar to that of a rigid sphere of radius a in a medium of viscosity η. The magnitudes of the vectors between nuclei of a rigid sphere remain fixed and the average values $\langle r_{jj}^{-6} \rangle$ and $\langle r_{jk}^{-6} \rangle$ of eq.(3.12) are replaced by r_{jj}^{-6} and r_{jk}^{-6} respectively. The correlation times $(\tau_c)_{jj}$ and $(\tau_c)_{jk}$ are assumed to be equal for a sphere and may be replaced by a single time $(\tau_c)_{dd}$. This correlation time is of the order of the time involved for a molecule to turn through a radian and is generally extremely short such that $\omega^2(\tau_c)_{dd}^2 << 1$ (Andrew 1955, p. 116). Using this approximation in eq.(3.12) and making the substitutions indicated above, the intramolecular dipole-dipole contribution can be written as

$$(1/T_1)_{dd\text{-}intra} = \hbar^2\gamma_j^2\Big[2I_j(I_j+1)\gamma_j^2 \sum_j r_{jj}^{-6} + (4/3)\sum_k I_k(I_k+1)\gamma_k^2 r_{jk}^{-6}\Big](\tau_c)_{dd} \qquad (3.14)$$

where the correlation time $(\tau_c)_{dd}$ is given by Bloembergen et al. (1948) to be

$$(\tau_c)_{dd} = 4\pi\eta a^3/3kT \quad . \qquad (3.15)$$

3.1.2 Intermolecular Dipole-Dipole Contribution

Consider a nucleus j interacting with nuclei in different molecules contained in a spherical shell between r and r+dr, where the center of the shell is located at the center of the molecule to which the nucleus j belongs. Assuming translational motion of the molecules to be diffusion-like, the translational correlation time may be expressed in terms of the diffusion coefficient D of the liquid and Bloembergen et al. (1948) give that

$$(\tau_c)_{transl} = r^2/12D \qquad (3.16)$$

where r is the distance a particular molecule of the shell moves relative to the molecule containing the nucleus j in the time $(\tau_c)_{transl}$. According to eq.(3.16) the correlation time $(\tau_c)_{transl}$ increases with increasing values of r, and the approximation $\left[\omega^2(\tau_c)^2_{transl} << 1\right]$ may also be used here because neighbors with large r will have no appreciable effect on nucleus j due to the factors r^{-6} in eq.(3.12).

Thus far molecules in the shell or element of volume $4\pi r^2 dr$ have been considered. The effects of all neighbors are taken into account by integrating over the volume from ∞ to the distance of closest approach which is written as d_{jj} for j-j nuclei and d_{jk} for j-k nuclei. Letting N to be the number of molecules per cm^3, the total intermolecular

dipole-dipole contribution is found by multiplying the integration over the volume by N. Then, letting $(\tau_c)_{jj} = (\tau_c)_{jk} = (\tau_c)_{transl}$, eq.(3.12) becomes the following

$$(1/T_1)_{dd\text{-}inter} = \hbar^2\gamma_j^2 N\Big[2I_j(I_j+1)\gamma_j^2\sum_j\int_{\infty}^{d_{jj}} r_{jj}^{-6}(r^2/12D)\,4\pi r^2 dr$$

$$+ (4/3)\sum_k I_k(I_k+1)\gamma_k^2\int_{\infty}^{d_{jk}} r_{jk}^{-6}(r^2/12D)\,4\pi r^2 dr\Big]$$

$$= (\pi\hbar^2\gamma_j^2 N/D)\Big[(2/3)I_j(I_j+1)\gamma_j^2\sum_j d_{jj}^{-1}$$

$$+ (4/9)\sum_k I_k(I_k+1)\gamma_k^2 d_{jk}^{-1}\Big] \qquad (3.17)$$

where the summations are carried out over a single neighboring molecule only. The coefficient of self-diffusion, D, may be replaced by the well known Stokes-Einstein formula

$$D = kT/6\pi\eta a \quad . \qquad (3.18)$$

3.2 Spin-Rotational Contribution

A nucleus, besides interacting with the magnetic fields due to other nuclear dipoles, can also interact with the magnetic field resulting from the electric currents

set up by molecular rotation. The Hamiltonian describing this interaction may be written

$$\mathcal{H} = \bar{I} \cdot C \cdot \bar{J} \qquad (3.19)$$

where $\bar{I}$ is the nuclear spin,

C is a tensor,

$\bar{J}$ is the angular momentum of the molecule.

Due to molecular collisions $\bar{J}$ does not remain constant. The magnetic field at the nucleus j changes due to molecular rotation. Huntress (1968) has given the following expression for the relaxation rate involved here

$$(1/T_1)_{sr} = (2/3)kT \sum_{i=x,y,z} \left[C_{ii}^2 - 2C_{tr}(C_{ii}-C_{tr})\right] I_i (\tau_J)_i \qquad (3.20)$$

where x-y-z is a co-ordinate system fixed in the molecule,

C_{ii} are spin-rotation constants,

C_{tr} equals 1/3 of trace of the spin-rotation tensor,

I_i is the moment of inertia about the ith axis,

$(\tau_J)_i$ is an angular-velocity correlation time for the ith axis which can be written as $D_i I_i/kT$ where D_i is a quantity known as the rotational diffusion constant for the ith axis.

3.3 Quadrupolar Contribution

Nuclei having a spin $I > 1/2$ possess an electric quadrupole moment. Such a quadrupole moment can interact with the electric fields at the site of the nucleus. Due to molecular motions these fields are fluctuating rapidly resulting in transitions between the unperturbed magnetic energy levels. The Hamiltonian representing this interaction may be written in a similar form as that for the magnetic dipole case, i.e. eq.(3.4), and is given by (Pound 1950; Shimizu 1964)

$$\mathcal{H}_q = \frac{(eq)eQ}{2I(2I-1)} \left[2I_z^2 - (1/2)I^+I^- - (1/2)I^-I^+\right]f^0$$

$$+ (3/2)^{1/2}(I^+I_z + I_zI^+)f^{-1} + (3/2)^{1/2}(I^-I_z + I_zI^-)f^{+1}$$

$$+ (3/2)^{1/2}(I^+)^2f^{-2} + (3/2)^{1/2}(I^-)^2f^{+2} \qquad (3.21)$$

where e is the electronic charge,

Q is the quadrupole moment,

(eq) is the electric-field gradient,

$I^{\pm}$, I_z are the spin operators,

f^0, $f^{\pm 1}$, $f^{\pm 2}$ are position functions given by

$$f^0 = (1/4)(3\cos^2\theta - 1)$$

$$f^{\pm 1} = (3/8)^{1/2}\sin\theta\cos\theta\exp(\pm i\phi) \qquad (3.22)$$

$$f^{\pm 2} = (3/32)^{1/2}\sin^2\theta\exp(\pm 2i\phi)$$

with polar and azimuthal angles θ and ϕ respectively.

As in the case of dipolar interactions spectral densities are defined, giving the intensities of the Fourier spectra of the position functions. These spectral densities can be calculated using eqs.(3.6), (3.7) and (3.22). The relaxation rate due to quadrupolar interaction can be evaluated using the density matrix formulism and is given by the following expression (Shimizu 1964; Huntress 1968)

$$(1/T_1)_q = \frac{3\pi^2(2I+3)}{10I^2(2I-1)}(e^2qQ/h)^2(\tau_c)_q \qquad (3.23)$$

where $(\tau_c)_q$ is the correlation time associated with the reorientation of the electric-field gradient,

(e^2qQ/h) is the quadrupole coupling constant,

and $\omega^2(\tau_c)_q^2 << 1$.

For symmetric top molecules, $(\tau_c)_q$ is given by the following equation (Woessner 1962; Huntress 1968)

$$(\tau_c)_q = \frac{(1/4)(3\cos^2\theta-1)^2}{6D_\perp} + \frac{3\sin^2\theta\cos^2\theta}{5D_\perp + D_{//}} + \frac{(3/4)\sin^4\theta}{2D_\perp + 4D_{//}} \qquad (3.24)$$

where θ is the angle between the internuclear vector (symmetry axis of electric field) and the

motional symmetry axis of the molecule,

$D_{//}$ and $D_{\perp}$ are the rotational diffusion constants for rotation about and perpendicular to the motional symmetry axis respectively.

Substituting eq.(3.24) into eq.(3.23) gives

$$(1/T_1)_q = \frac{3\pi^2(2I+3)}{10I^2(2I-1)}(e^2qQ/h)^2\left[\frac{(1/4)(3\cos^2\theta-1)^2}{6D_{\perp}}\right.$$

$$\left. + \frac{3\sin^2\theta\cos^2\theta}{5D_{\perp} + D_{//}} + \frac{(3/4)\sin^4\theta}{2D_{\perp} + 4D_{//}}\right] . \qquad (3.25)$$

It may be noted that the relaxation rate given by eq.(3.25) represents the contribution due to the rotational motion of the molecule. It is well known (Shimizu 1964; Bonera and Rigamonti 1965b; Bopp 1967; Huntress 1968; Jonas and DiGennaro 1969) that the electric field at the nucleus due to other molecules in the liquid contribute negligibly to the relaxation and thus no intermolecular quadrupolar contribution need be considered.

The total relaxation rate can be expressed by adding the contributions evaluated in eqs.(3.14), (3.17), (3.20) and (3.25) and is given by

$$(1/T_1)_{total} = (1/T_1)_{dd\text{-}intra} + (1/T_1)_{dd\text{-}inter}$$

$$+ (1/T_1)_{sr} + (1/T_1)_q \ . \qquad (3.26)$$

3.4 Separation of Contributions

Measurements of T_1 made in a liquid yield only the left hand side of eq.(3.26), the total relaxation rate. One can only calculate the individual contributions using the expressions given earlier and then compare the sum of the calculated contributions with the experimental value. Unfortunately this can result in some misleading conclusions. Furthermore these individual contributions are sometimes difficult to calculate because the values of certain parameters required for the calculations are not available. Therefore it is desirable to separate the individual contributions experimentally in order to check the experimental results and gain some information about molecular motion.

The quadrupolar contribution can be eliminated by measuring T_1 of nuclei with spin 1/2. Since the intermolecular dipole-dipole contribution depends upon the number of molecules in the pure liquid, it is possible to separate this contribution from the others by studying T_1 of the liquid (solute) as a function of concentration in a magnetically neutral liquid or the perdeuterated analog (solvent) as long as the molecular motions of the solute molecules in the mixture do not differ from those in the pure solute and there are no molecular associations between

the solute and the solvent or an exchange of protons and deuterons between the liquid and its perdeuterated analog.

T_1 for a liquid (solute) in solution with another liquid (solvent) can be expressed as (Mitchell and Eisner 1960; Bonera and Rigamonti 1965a; Powles and Figgins 1966)

$$(1/T_1)_{expt.} = (1/T_1)_{intra} + f(1/T_1)_{dd\text{-}inter} + (1-f)(1/T_1)'_{dd\text{-}inter} \quad (3.27)$$

where $$(1/T_1)_{intra} = (1/T_1)_{dd\text{-}intra} + (1/T_1)_{sr} \quad (3.28)$$

f is the mole fraction of the solute molecules,

$(1/T_1)'_{dd\text{-}inter}$ is the contribution due to the solvent when a solute molecule is totally surrounded by solvent molecules.

By extrapolating the plot of $(1/T_1)_{expt.}$ versus f to f = 0 and subtracting $(1/T_1)'_{dd\text{-}inter}$ from the intercept, $(1/T_1)_{intra}$ is obtained. By subtracting $(1/T_1)_{intra}$ from $(1/T_1)_{expt.}$ in the pure solute, i.e. f = 1, $(1/T_1)_{dd\text{-}inter}$ is obtained.

For spherical molecules undergoing isotropic rotational diffusion, $(1/T_1)_{dd\text{-}intra}$ and $(1/T_1)_{sr}$ can be separated from $(1/T_1)_{intra}$ by using the expression (Smith and Powles 1966; Powles and Figgins 1966; Woessner et al.1968)

$$(1/T_1)_{dd\text{-}intra}\ (1/T_1)_{sr} = (1/4)(1/T_1)^{min}_{intra} \quad (3.29)$$

where $(1/T_1)^{min}_{intra}$ is the minimum value of the intramolecular relaxation rate. Using eqs.(3.28) and (3.29), $(1/T_1)_{dd\text{-}intra}$ and $(1/T_1)_{sr}$ can be seperated.

For nonspherical molecules, $(1/T_1)_{dd\text{-}intra}$ and $(1/T_1)_{sr}$ can be seperated by calculating $(1/T_1)_{dd\text{-}intra}$ using eq.(3.14), where $(\tau_c)_{dd}$ has been replaced by correlation times pertinent to the individual internuclear vectors (Woessner et al. 1968; Gillen et al. 1971). Subtracting this calculated value of $(1/T_1)_{dd\text{-}intra}$ from $(1/T_1)_{intra}$ gives $(1/T_1)_{sr}$. The correlation times used in place of $(\tau_c)_{dd}$ of eq.(3.14) are evaluated from eq.(3.24) using the appropriate angles between the symmetry axis of the molecule and the internuclear vectors joining the i-j nuclei and i-k nuclei. $(1/T_1)_{dd\text{-}intra}$ may thus be evaluated using physical constants, known internuclear distances and bond angles, and the rotational diffusion constants $D_\perp$ and $D_{//}$. $D_\perp$ and $D_{//}$ can be calculated by obtaining $(\tau_c)_q$'s from a study of T_1 of two different quadrupolar nuclei, i.e. eq.(3.23), and substituting these values of $(\tau_c)_q$ into eq.(3.24).

CHAPTER 4

EXPERIMENTAL RESULTS AND DISCUSSION

Measurements of T_1 were performed at a frequency of 4 Mc/sec in pure (oxygen-free) liquid samples of CH_2I_2, CD_2I_2, and CH_2I_2 - CD_2I_2 mixtures, using the method described in sec.(2.4). The samples were purified using the technique described in sec.(2.3). Before presenting the measurements of T_1, a brief description of the methylene iodide (CH_2I_2) molecule is given.

4.1 CH_2I_2 Molecule

The arrangement of the various nuclei in the CH_2I_2 molecule is shown in Fig. 11 and some of its geometric parameters are given in Table I. This molecule belongs to the C_{2v} point group (Herzberg 1945, p. 6) and thus has a twofold axis of symmetry (Y-axis, Fig. 11) as well as two mutually perpendicular planes of symmetry (planes HCH and ICI, Fig. 11). Molecules of the C_{2v} point group are considered to be asymmetric top molecules, but if two of the principal moments of inertia are equal, the molecule is taken to be a symmetric top molecule (Herzberg 1945, p. 13). Using the atomic masses of the atoms of this molecule and interatomic distances given in Appendix B, the principal moments of inertia about the center of mass are calculated to be $I_X = 13.77 \times 10^{-38}$ g-cm^2, $I_Y = 13.45 \times 10^{-38}$ g-cm^2 and $I_Z = 0.374 \times 10^{-38}$ g-cm^2. Thus this molecule is taken

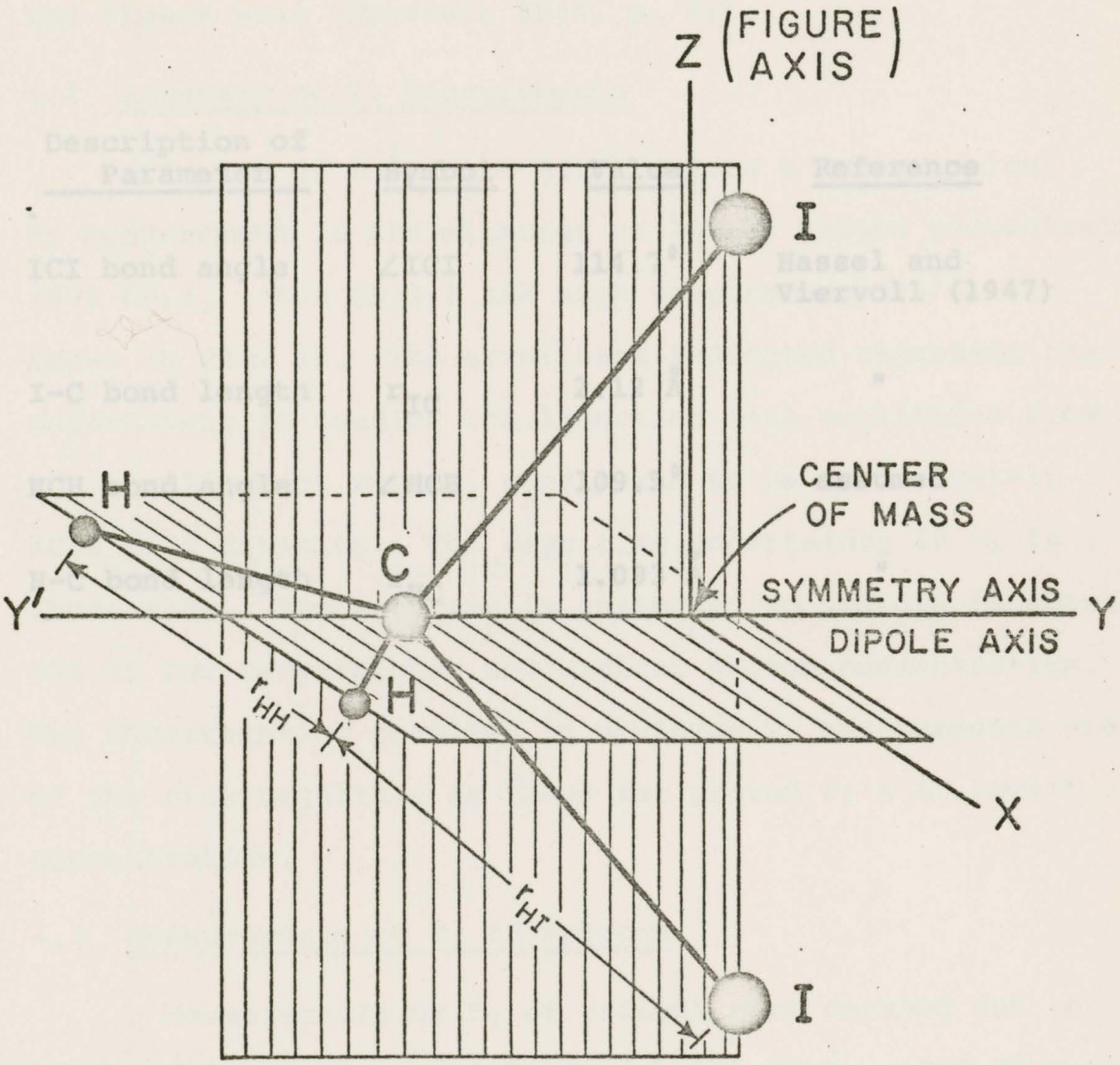

Fig. 11 CH_2I_2 molecule

TABLE I Geometric Parameters of the CH_2I_2 Molecule

Description of Parameter	Symbol	Value	Reference
ICI bond angle	$\angle ICI$	114.7^0	Hassel and Viervoll (1947)
I-C bond length	r_{IC}	2.12 Å	"
HCH bond angle	$\angle HCH$	109.5^0	assumed
H-C bond length	r_{HC}	1.093 Å	"

to be a symmetric top molecule (i.e. since $I_X \simeq I_Y$). The Z-axis (Fig. 11), about which the moment of inertia is different from the other two moments of inertia is known as the figure axis (Herzberg 1945, p. 22).

4.2 Accuracy of T_1 Measurements

A plot of $\ln\left[A(\infty) - A(t)\right]$ versus t for a typical T_1 measurement in the mixtures at lowest proton concentration (40% CH_2I_2 - 60% CD_2I_2) and high temperature (95°C) is shown in Fig. 12. The error bars indicated represent the uncertainty in reading the induction tail amplitudes from the oscilloscope screen, considered to be approximately ±0.2 of a division. The resulting uncertainty in T_1 is about ±10%. The accuracy is estimated to improve to about ±5% at low temperatures and highest proton concentration. The uncertainties involved in deuteron T_1 measurements are of the same magnitude as those for proton T_1's at lowest concentration.

4.3 Measurements of T_1 of Protons

Measurements of T_1 of protons were carried out in oxygen-free samples of 100% CH_2I_2, 80% CH_2I_2 - 20% CD_2I_2, 60% CH_2I_2 - 40% CD_2I_2 and 40% CH_2I_2 - 60% CD_2I_2, by volume, between 7 - 100°C and the results are plotted as $\ln(1/T_1)$ versus $1000/T^0K$ in Fig. 13. The straight lines passing through the data are obtained by the method of least squares. T_1 in pure CH_2I_2 has been previously measured

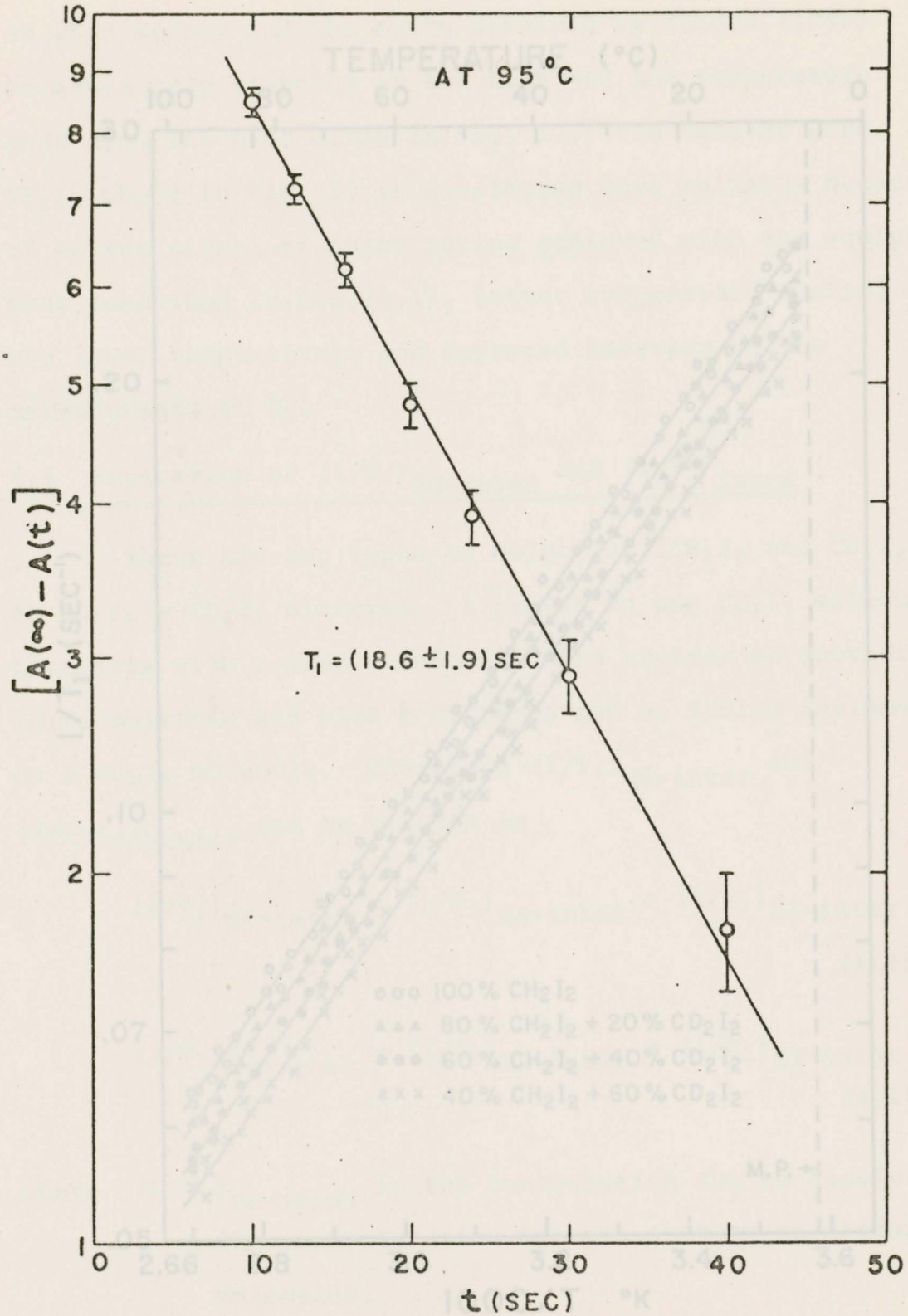

Fig. 12 A typical plot of $\ln\left[A(\infty) - A(t)\right]$ versus t

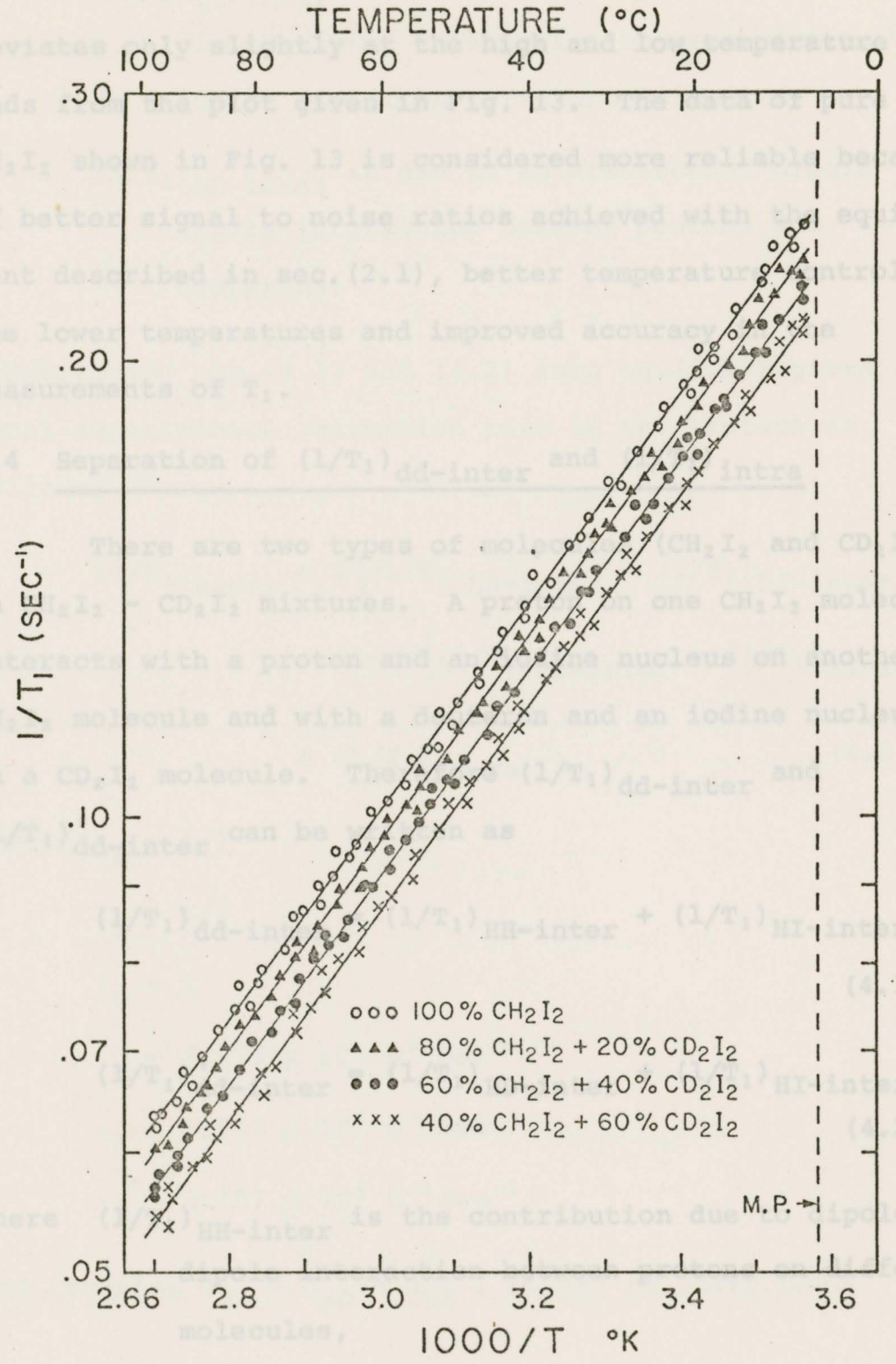

Fig. 13 Plot of $\ln(1/T_1)$ of protons versus $1000/T^{\circ}K$ in CH_2I_2 - CD_2I_2 mixtures

at 26.8 Mc/sec and the curve obtained by Sandhu (1969) deviates only slightly at the high and low temperature ends from the plot given in Fig. 13. The data of pure CH_2I_2 shown in Fig. 13 is considered more reliable because of better signal to noise ratios achieved with the equipment described in sec.(2.1), better temperature control at the lower temperatures and improved accuracy in the measurements of T_1.

4.4 Separation of $(1/T_1)_{dd\text{-}inter}$ and $(1/T_1)_{intra}$

There are two types of molecules (CH_2I_2 and CD_2I_2) in CH_2I_2 - CD_2I_2 mixtures. A proton on one CH_2I_2 molecule interacts with a proton and an iodine nucleus on another CH_2I_2 molecule and with a deuteron and an iodine nucleus on a CD_2I_2 molecule. Therefore $(1/T_1)_{dd\text{-}inter}$ and $(1/T_1)'_{dd\text{-}inter}$ can be written as

$$(1/T_1)_{dd\text{-}inter} = (1/T_1)_{HH\text{-}inter} + (1/T_1)_{HI\text{-}inter} \tag{4.1}$$

$$(1/T_1)'_{dd\text{-}inter} = (1/T_1)_{HD\text{-}inter} + (1/T_1)_{HI\text{-}inter} \tag{4.2}$$

where $(1/T_1)_{HH\text{-}inter}$ is the contribution due to dipole-dipole interaction between protons on different molecules,

$(1/T_1)_{HI\text{-}inter}$ is the contribution arising from dipole-dipole interaction between protons and iodine nuclei on different molecules,

$(1/T_1)_{HD\text{-}inter}$ is due to intermolecular dipole-dipole interaction between protons and deuterons.

Substituting eqs.(4.1) and (4.2) into eq.(3.27) gives the total experimental relaxation rate in the mixture as follows:

$$(1/T_1)_{expt.} = f\left[(1/T_1)_{HH\text{-}inter} + (1/T_1)_{HI\text{-}inter}\right] + (1-f)\left[(1/T_1)_{HD\text{-}inter} + (1/T_1)_{HI\text{-}inter}\right] + (1/T_1)_{intra} \quad . \qquad (4.3)$$

Taking $I_H = 1/2$

$I_I = 5/2$

$I_D = 1$

$\gamma_H = 2.675 \times 10^4 \ G^{-1}sec^{-1}$

$\gamma_I = 5.353 \times 10^3 \ G^{-1}sec^{-1}$

$\gamma_D = 4.107 \times 10^3 \ G^{-1}sec^{-1}$

and assuming $d_{HH} = d_{HD} = d_{HI}$, it can be shown that

$$\frac{(1/T_1)_{HD\text{-}inter}}{(1/T_1)_{HH\text{-}inter}} = \frac{2I_D(I_D+1)\gamma_D^2 \sum_D d_{HD}^{-1}}{3I_H(I_H+1)\gamma_H^2 \sum_H d_{HH}^{-1}} = 0.042 \qquad (4.4a)$$

$$\frac{(1/T_1)_{HI\text{-}inter}}{(1/T_1)_{HH\text{-}inter}} = \frac{2I_I(I_I+1)\gamma_I^2 \sum_I d_{HI}^{-1}}{3I_H(I_H+1)\gamma_H^2 \sum_H d_{HH}^{-1}} = 0.311 \qquad (4.4b)$$

Equation (4.4) can be written as

$$(1/T_1)_{HD\text{-}inter} = 0.042(1/T_1)_{HH\text{-}inter} \qquad (4.5a)$$

$$(1/T_1)_{HI\text{-}inter} = 0.311(1/T_1)_{HH\text{-}inter} \; . \qquad (4.5b)$$

Substituting eq.(4.5) into eq.(4.3) gives

$$(1/T_1)_{expt.} = (0.958f + 0.353)(1/T_1)_{HH\text{-}inter} + (1/T_1)_{intra} \; .$$

It is convenient to express this equation as

$$(1/T_1)_{expt.} = (1/T_1)_{HH\text{-}inter}(23/24)f + \left[0.353(1/T_1)_{HH\text{-}inter} + (1/T_1)_{intra}\right]. \qquad (4.6)$$

It can be seen that the slope and the intercept of the plot

of $(1/T_1)_{expt.}$ versus $(23/24)f$ gives

$$\text{SLOPE} = (1/T_1)_{HH\text{-inter}}$$

$$\text{INTERCEPT} = 0.353(1/T_1)_{HH\text{-inter}} + (1/T_1)_{intra}$$

$$= 0.353\ \text{SLOPE} + (1/T_1)_{intra}$$

or $$(1/T_1)_{HH\text{-inter}} = \text{SLOPE} \qquad (4.7)$$

$$(1/T_1)_{intra} = \text{INTERCEPT} - 0.353\ \text{SLOPE} \ . \qquad (4.8)$$

A plot of $(1/T_1)_{expt.}$ versus $(23/24)f$ at 25^0C is shown in Fig. 14. The error bars indicated in Fig. 14 represent the standard deviations of the $(1/T_1)_{expt.}$ values calculated by the method of least squares. It can be seen that the plot is a straight line whose intercept and slope, using eqs.(4.7) and (4.8), give $(1/T_1)_{HH\text{-inter}}$ and $(1/T_1)_{intra}$. $(1/T_1)_{dd\text{-inter}}$, obtained by combining eqs.(4.7), (4.5b) and (4.1), is given by

$$(1/T_1)_{dd\text{-inter}} = 1.311\ \text{SLOPE} \ . \qquad (4.9)$$

$(1/T_1)_{intra}$ and $(1/T_1)_{dd\text{-inter}}$ are evaluated using the approach outlined above and are plotted as $\ln(1/T_1)_{intra}$ and $\ln(1/T_1)_{dd\text{-inter}}$ against $1000/T^0K$ in Fig. 15. The computer program used for these calculations is given in Appendix A (Program I). It can be seen that the plots are straight lines and the two contributions increase with

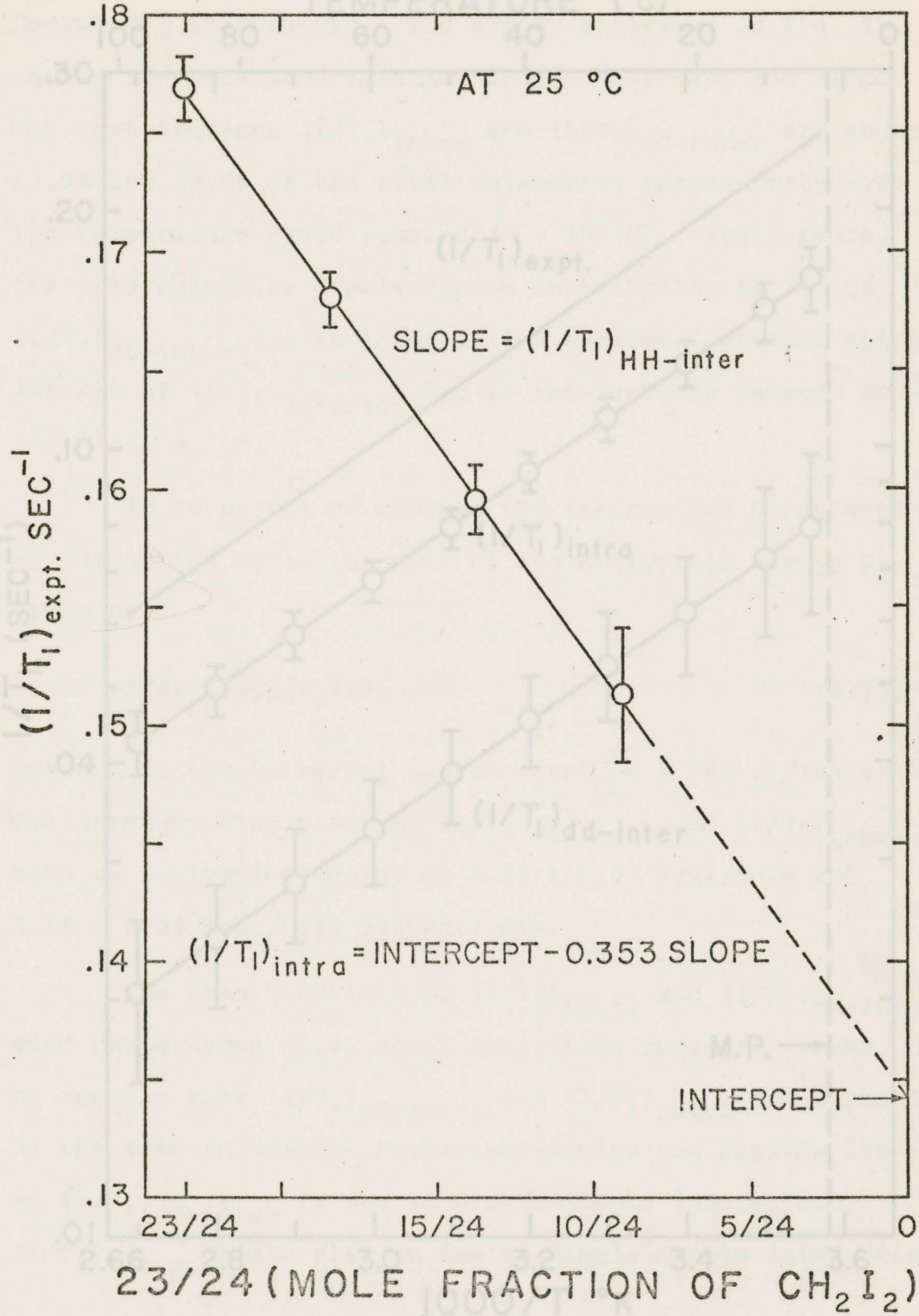

Fig. 14 Typical plot of $(1/T_1)_{expt.}$ versus (23/24) (mole fraction of CH_2I_2)

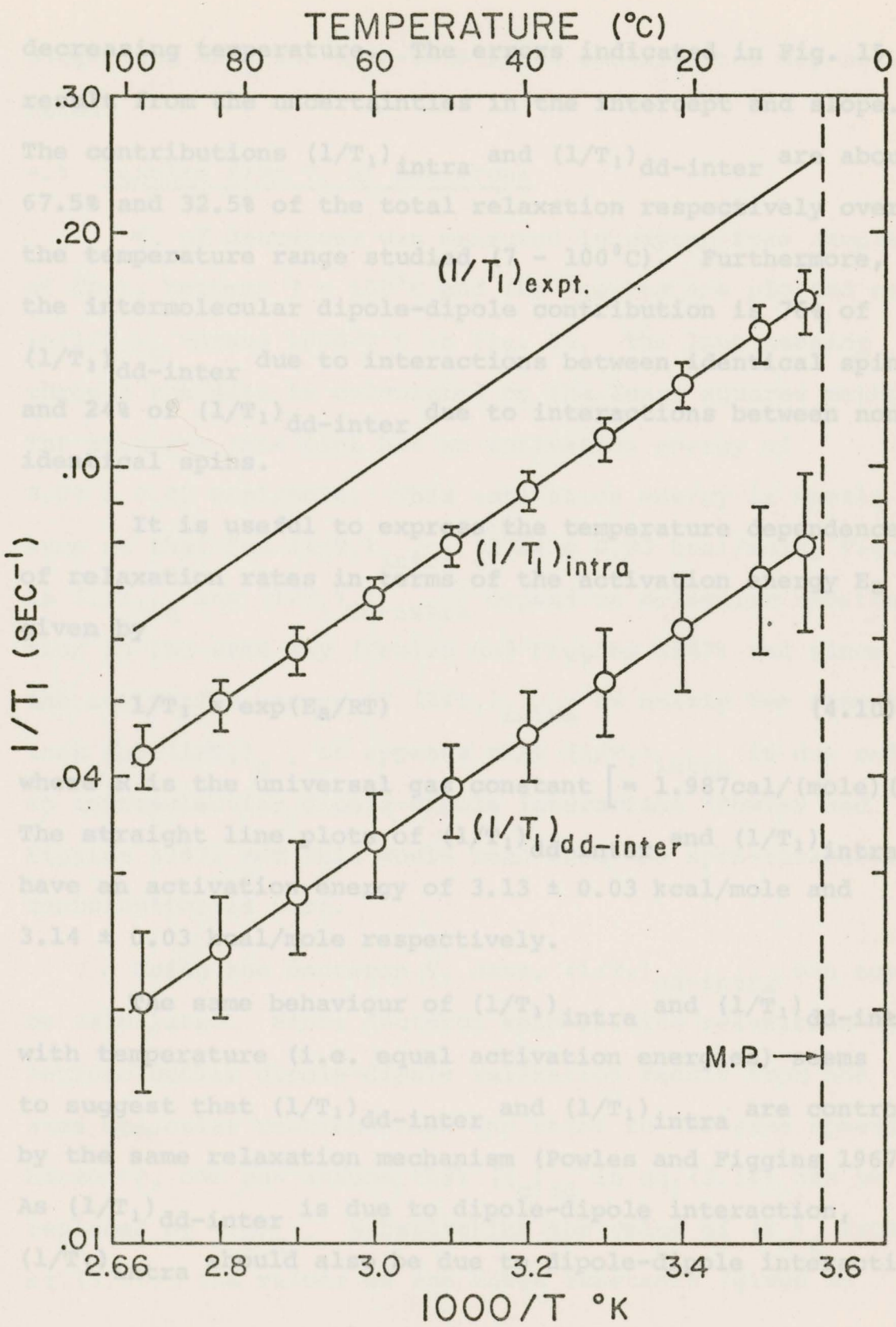

Fig. 15 Plots of $\ln(1/T_1)_{expt.}$, $\ln(1/T_1)_{intra}$, and $\ln(1/T_1)_{dd\text{-}inter}$ versus $1000/T^0K$

decreasing temperature. The errors indicated in Fig. 15 result from the uncertainties in the intercept and slope. The contributions $(1/T_1)_{intra}$ and $(1/T_1)_{dd\text{-}inter}$ are about 67.5% and 32.5% of the total relaxation respectively over the temperature range studied (7 - 100°C). Furthermore, the intermolecular dipole-dipole contribution is 76% of $(1/T_1)_{dd\text{-}inter}$ due to interactions between identical spins and 24% of $(1/T_1)_{dd\text{-}inter}$ due to interactions between non-identical spins.

It is useful to express the temperature dependence of relaxation rates in terms of the activation energy E_a given by

$$1/T_1 \propto \exp(E_a/RT) \qquad (4.10)$$

where R is the universal gas constant $\left[= 1.987 \text{cal}/(\text{mole})\,(^0\text{K})\right]$. The straight line plots of $(1/T_1)_{dd\text{-}inter}$ and $(1/T_1)_{intra}$ have an activation energy of 3.13 ± 0.03 kcal/mole and 3.14 ± 0.03 kcal/mole respectively.

The same behaviour of $(1/T_1)_{intra}$ and $(1/T_1)_{dd\text{-}inter}$ with temperature (i.e. equal activation energies) seems to suggest that $(1/T_1)_{dd\text{-}inter}$ and $(1/T_1)_{intra}$ are controlled by the same relaxation mechanism (Powles and Figgins 1967). As $(1/T_1)_{dd\text{-}inter}$ is due to dipole-dipole interaction, $(1/T_1)_{intra}$ should also be due to dipole-dipole interaction,

suggesting that the spin-rotational contribution may be zero.

4.5 Results from T_1 of Deuterons

T_1 of deuterons was measured in oxygen-free samples of CD_2I_2 between 7 - 100°C and the results are plotted as $\ln(1/T_1)_q$ versus $1000/T^0K$ in Fig. 16. The line passing through the data is calculated by the least squares method. The straight line plot has an activation energy of 3.07 ± 0.02 kcal/mole. This activation energy is nearly the same as that for $(1/T_1)_{intra}$ [3.14 ± 0.03 kcal/mole, Fig. 15]. As $(1/T_1)_q$ and $(1/T_1)_{dd\text{-}intra}$ depend on molecular reorientation in the same way (Powles and Figgins 1967) and since the activation energy of $(1/T_1)_{intra}$ is nearly the same as that for $(1/T_1)_q$, it appears that $(1/T_1)_{intra}$ is due only to intramolecular dipole-dipole interaction (Powles and Figgins 1967) and this would mean that the spin-rotational contribution is zero.

Using the deuteron T_1 data, $(1/T_1)_{dd\text{-}intra}$ can now be calculated. Since deuteron spin-lattice relaxation and intramolecular dipole-dipole relaxation result from the same molecular reorientation and refer to the same spherical harmonic, one can assume that $(\tau_c)_{dd}$ in eq.(3.14) can be replaced by $(\tau_c)_q$. Substituting the value of $(\tau_c)_q$ from eq.(3.23), the values of the known constants (given on

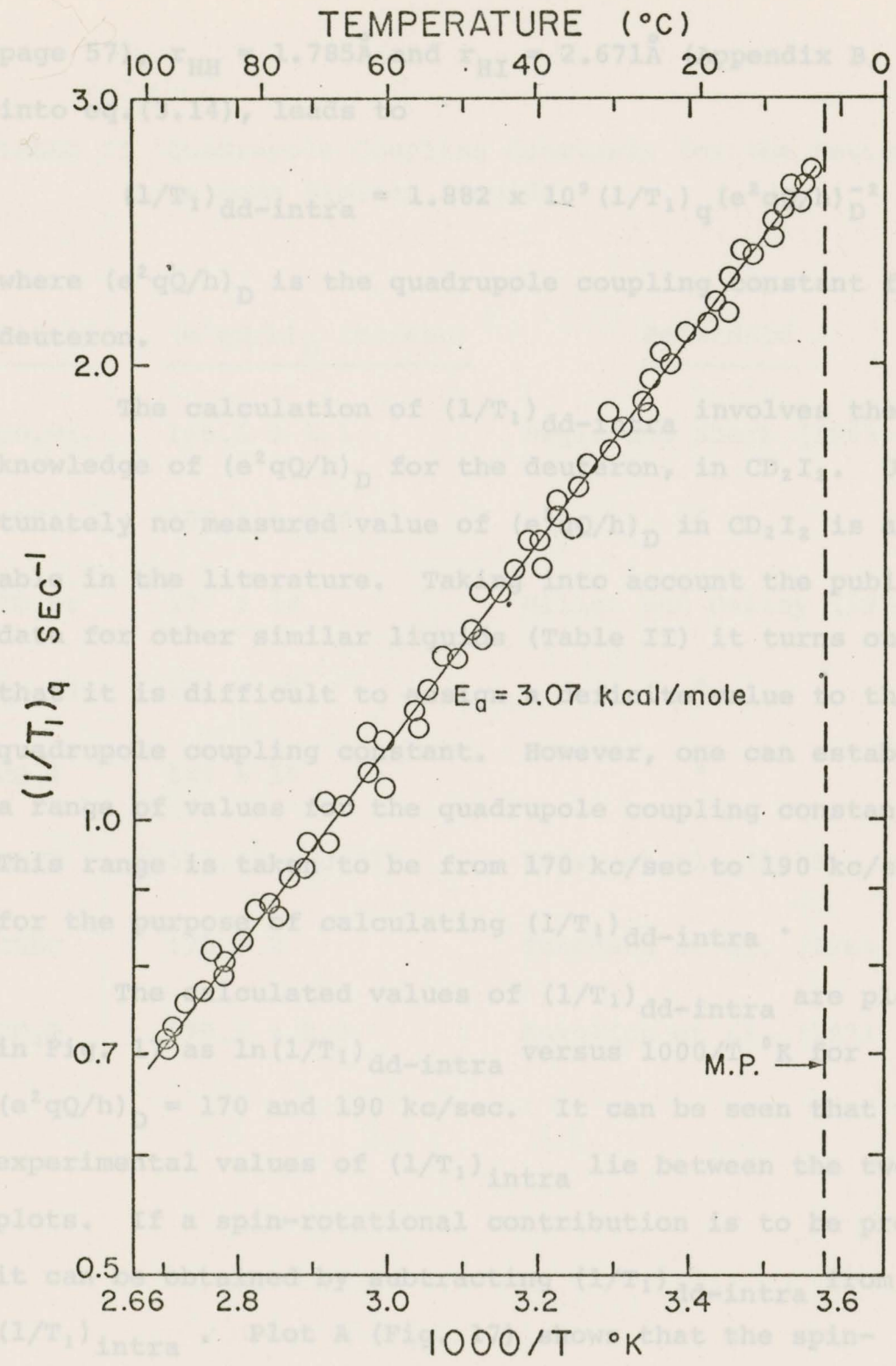

Fig. 16 Plot of $\ln(1/T_1)_q$ of deuterons versus $1000/T^0K$ in liquid CD_2I_2

page 57), $r_{HH} = 1.785\text{Å}$ and $r_{HI} = 2.671\text{Å}$ (Appendix B, eq.B.5) into eq.(3.14), leads to

$$(1/T_1)_{dd\text{-}intra} = 1.882 \times 10^9 (1/T_1)_q (e^2qQ/h)_D^{-2} \quad (4.11)$$

where $(e^2qQ/h)_D$ is the quadrupole coupling constant for the deuteron.

The calculation of $(1/T_1)_{dd\text{-}intra}$ involves the knowledge of $(e^2qQ/h)_D$ for the deuteron, in CD_2I_2. Unfortunately no measured value of $(e^2qQ/h)_D$ in CD_2I_2 is available in the literature. Taking into account the published data for other similar liquids (Table II) it turns out that it is difficult to assign a definite value to the quadrupole coupling constant. However, one can establish a range of values for the quadrupole coupling constant. This range is taken to be from 170 kc/sec to 190 kc/sec for the purpose of calculating $(1/T_1)_{dd\text{-}intra}$.

The calculated values of $(1/T_1)_{dd\text{-}intra}$ are plotted in Fig. 17 as $\ln(1/T_1)_{dd\text{-}intra}$ versus $1000/T\ ^0K$ for $(e^2qQ/h)_D = 170$ and 190 kc/sec. It can be seen that the experimental values of $(1/T_1)_{intra}$ lie between the two plots. If a spin-rotational contribution is to be present, it can be obtained by subtracting $(1/T_1)_{dd\text{-}intra}$ from $(1/T_1)_{intra}$. Plot A (Fig. 17) shows that the spin-rotational contribution is zero for $(e^2qQ/h)_D = 170$ kc/sec.

TABLE II Quadrupole Coupling Constants for the Deuteron in Some Similar Liquids

Liquid	$(e^2qQ/h)_D$ (kc/sec)	Reference
CD_2Cl_2	169.6 ± 1.1	Ragle and Sherk (1969)
$CDCl_3$	167.6 ± 0.8	"
CD_3Br	177 ± 18	Millet and Dailey (1972)
CD_3CN	171 ± 17	"
CD_3I	189 ± 19	"
CH_3D	191.48 ± 0.077	Wofsy et al. (1970)
CHDO	170 ± 2	Thaddeus et al. (1964)
CF_3D	170.8 ± 2.0	Kukolich et al. (1971)

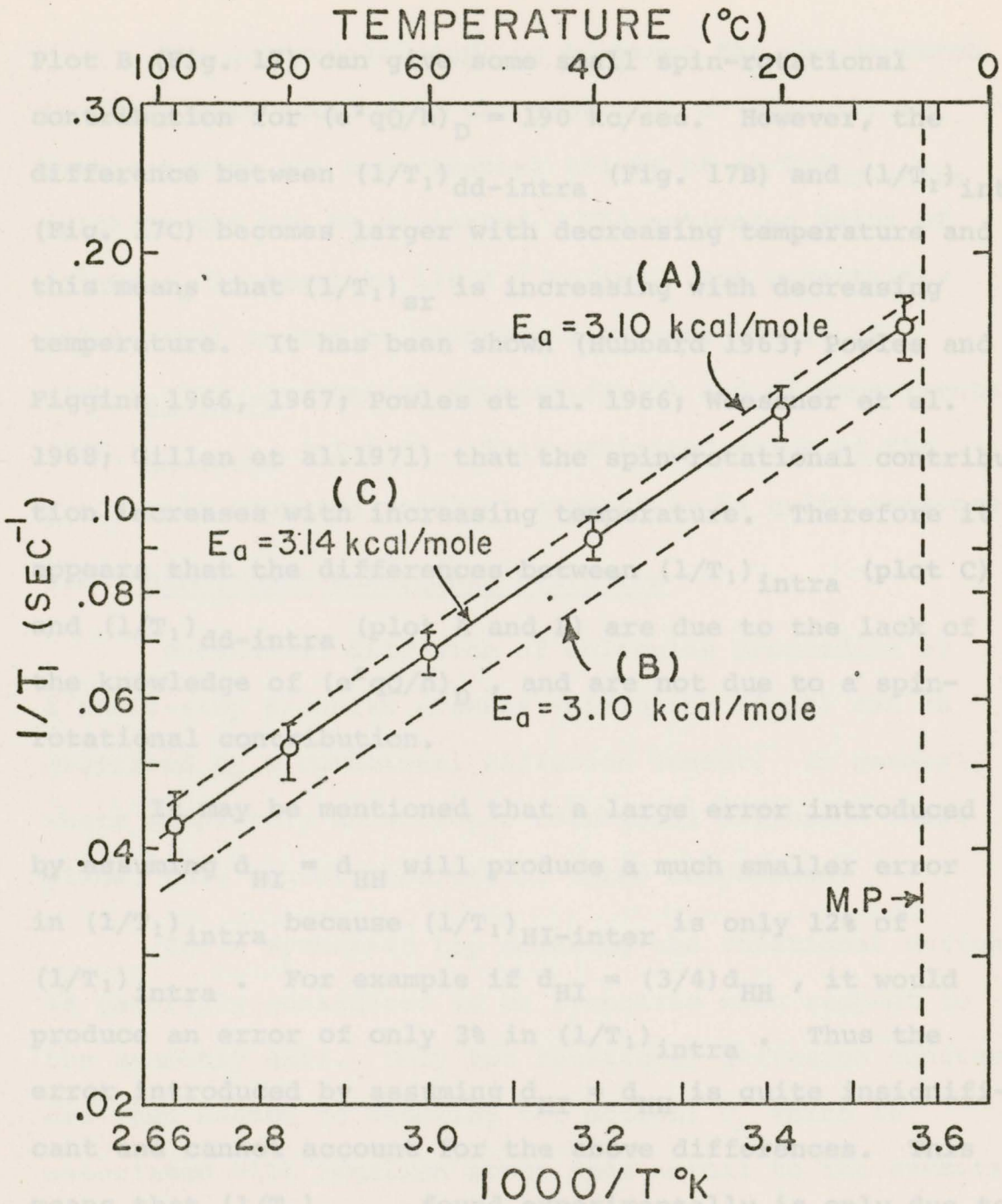

Fig. 17 Plots of $\ln(1/T_1)$ versus $1000/T^0K$;

plot (A) shows $(1/T_1)_{dd\text{-}intra}$ obtained using $(e^2qQ/h)_D$ = 170 kc/sec,

plot (B) shows $(1/T_1)_{dd\text{-}intra}$ obtained using $(e^2qQ/h)_D$ = 190 kc/sec,

plot (C) is the $(1/T_1)_{intra}$ line replotted from Fig. 15.

Plot B (Fig. 17) can give some small spin-rotational contribution for $(e^2qQ/h)_D$ = 190 kc/sec. However, the difference between $(1/T_1)_{dd\text{-}intra}$ (Fig. 17B) and $(1/T_1)_{intra}$ (Fig. 17C) becomes larger with decreasing temperature and this means that $(1/T_1)_{sr}$ is increasing with decreasing temperature. It has been shown (Hubbard 1963; Powles and Figgins 1966, 1967; Powles et al. 1966; Woessner et al. 1968; Gillen et al.1971) that the spin-rotational contribution increases with increasing temperature. Therefore it appears that the differences between $(1/T_1)_{intra}$ (plot C) and $(1/T_1)_{dd\text{-}intra}$ (plot A and B) are due to the lack of the knowledge of $(e^2qQ/h)_D$, and are not due to a spin-rotational contribution.

It may be mentioned that a large error introduced by assuming $d_{HI} = d_{HH}$ will produce a much smaller error in $(1/T_1)_{intra}$ because $(1/T_1)_{HI\text{-}inter}$ is only 12% of $(1/T_1)_{intra}$. For example if $d_{HI} = (3/4)d_{HH}$, it would produce an error of only 3% in $(1/T_1)_{intra}$. Thus the error introduced by assuming $d_{HI} = d_{HH}$ is quite insignificant and cannot account for the above differences. This means that $(1/T_1)_{intra}$ found experimentally is only due to dipole-dipole interaction, i.e. $(1/T_1)_{intra} = (1/T_1)_{dd\text{-}intra}$ and $(1/T_1)_{sr} = 0$. Here, from now on $(1/T_1)_{intra}$ will be referred to as $(1/T_1)_{dd\text{-}intra}$.

The quadrupole coupling constant for the deuteron in CD_2I_2 that would make the plot A or B (Fig. 17) to coincide with the experimental values of $(1/T_1)_{dd\text{-intra}}$ (plot C) can now be estimated. The estimated value of $(e^2qQ/h)_D$ is equal to 176 ± 2 kc/sec. The uncertainty (±2 kc/sec) is due to slightly different slopes of $(1/T_1)_{dd\text{-intra}}$ obtained from eq.(4.11) and of experimental $(1/T_1)_{dd\text{-intra}}$ (plot C). This estimated value of the quadrupole coupling constant appears to be quite reasonable.

4.6 Anisotropic Rotational Diffusion

Rotational diffusion of molecules proceeding by a small-step Brownian process (diffusion limit) can be described by a rotational diffusion tensor. In general, where completely anisotropic rotational diffusion takes place, this tensor consists of three components.

For a symmetric top molecule the rotational motion is generally considered to be symmetric with respect to the symmetry axis. Only two rotational diffusion constants are then needed to describe the motion; $D_\perp$ which is associated with rotation about axes normal to the symmetry axis and $D_{\parallel}$ which is associated with rotation about the symmetry axis. The CH_2I_2 molecule has a dipole moment equal to 6.2×10^{-18}esu (Prichard and Orville-Thomas 1963) and the dipole axis coincides with the molecule's symmetry axis YY' (Fig. 11). Due to the interactions among dipoles

it might be expected that the reorientation of the dipole axis proceeds much more slowly than the reorientation about the dipole axis. This suggests that the rotational motion of this molecule is symmetric with respect to its dipole axis (i.e. symmetry axis YY', Fig. 11). Therefore $D_{//}$ can be associated with motion about the symmetry axis and $D_{\perp}$ with motion about axes perpendicular to the symmetry axis.

One approach for finding $D_{\perp}$ and $D_{//}$ involves the study of T_1 of two different quadrupolar nuclei of a molecule and solving eq.(3.25) for $D_{\perp}$ and $D_{//}$. The CD_2I_2 molecule has two quadrupolar nuclei; the deuteron and iodine. However, the quadrupole coupling constant associated with the iodine nucleus is rather large (1897 Mc/sec, Robinson et al. 1954) and therefore the relaxation time of the iodine nucleus is quite small as indicated by eq.(3.23) and is not measurable. Thus one rotational diffusion constant needs to be determined by other means.

In certain cases, one of the rotational diffusion constants may be calculated from the Stokes rotational diffusion constant (D_{μ}) given by

$$D_{\mu} = kT/8\pi\eta a^3 \qquad (4.12)$$

where a is the radius of the molecules. The quantity η is the macroscopic viscosity which applies to molecules surrounded by layers of fluid, where the layers are of

infinitesmal thickness. In liquids a molecule is moving in a medium that consists of other molecules of finite size and thus the layer of fluid surrounding a molecule is of finite thickness. Taking into account the finite size of the molecules of the medium, Gierer and Wirtz (1953) introduced a microviscosity factor f_r for rotational motion and eq.(4.12) can be written as

$$D_\mu = kT/8\pi\eta a^3 f_r \ .$$

For a pure liquid $f_r = 1/6.125$,

$$\therefore D_\mu = 6.125kT/8\pi\eta a^3 \ . \qquad (4.13)$$

Assuming the molecules in the liquid have a hexagonally close-packed structure and thus fill only 0.74 of the available volume, the radius a is given by

$$(4/3)\pi a^3 N_o = 0.74M/d \qquad (4.14)$$

where N_o is Avogadro's number, M is the molecular weight and d is the density. Substituting eq.(4.14) in eq.(4.13) and taking

$$k = 1.38 \times 10^{-16} \text{erg}/^0\text{K}$$

$$N_o = 6.0225 \times 10^{23} \text{ molecules/mole}$$

$$M = 267.84 \text{ (for } CH_2I_2\text{)}$$

leads to

$$D_{\mu} = 4.28 \times 10^{5} Td/\eta \quad . \qquad (4.15)$$

Gillen and Noggle (1970) found that molecular motions in pure liquids which reorient an electric dipole are highly likely to be in the rotational diffusion limit and that in such cases $D_{\perp}$ may be calculated with good accuracy by taking $D_{\mu} = D_{\perp}$. Assuming that this also applies to the CH_2I_2 molecule eq.(4.15) can be rewritten as

$$D_{\perp} = 4.28 \times 10^{5} Td/\eta \quad . \qquad (4.16)$$

Equation (4.16) is evaluated using viscosity and density values given by Griffing et al. (1954) and is plotted as $\ln D_{\perp}$ versus $1000/T^{0}K$ in Fig. 18. This plot is a straight line with an activation energy of 3.09 kcal/mole.

$D_{//}$ is then calculated from eq.(3.25), taking I = 1, $D_{\perp}$ from Fig. 18, $(1/T_1)_q$ from Fig. 16 and $\theta = 54.75^{0}$, i.e. $(1/2)\angle HCH$. The computer program used for these calculations is given in Appendix A (Program IIA). Fig. 18 shows a plot of $\ln D_{//}$ versus $1000/T^{0}K$ for $(e^2qQ/h)_D$ = 176 kc/sec and it can be seen that this plot is a straight line with an activation energy of 3.10 kcal/mole.

Fig. 18 shows that $D_{//} \neq D_{\perp}$ which indicates that this molecule undergoes anisotropic rotational diffusion. The ratio $D_{//}/D_{\perp}$ is approximately 6.7 over the temperature range

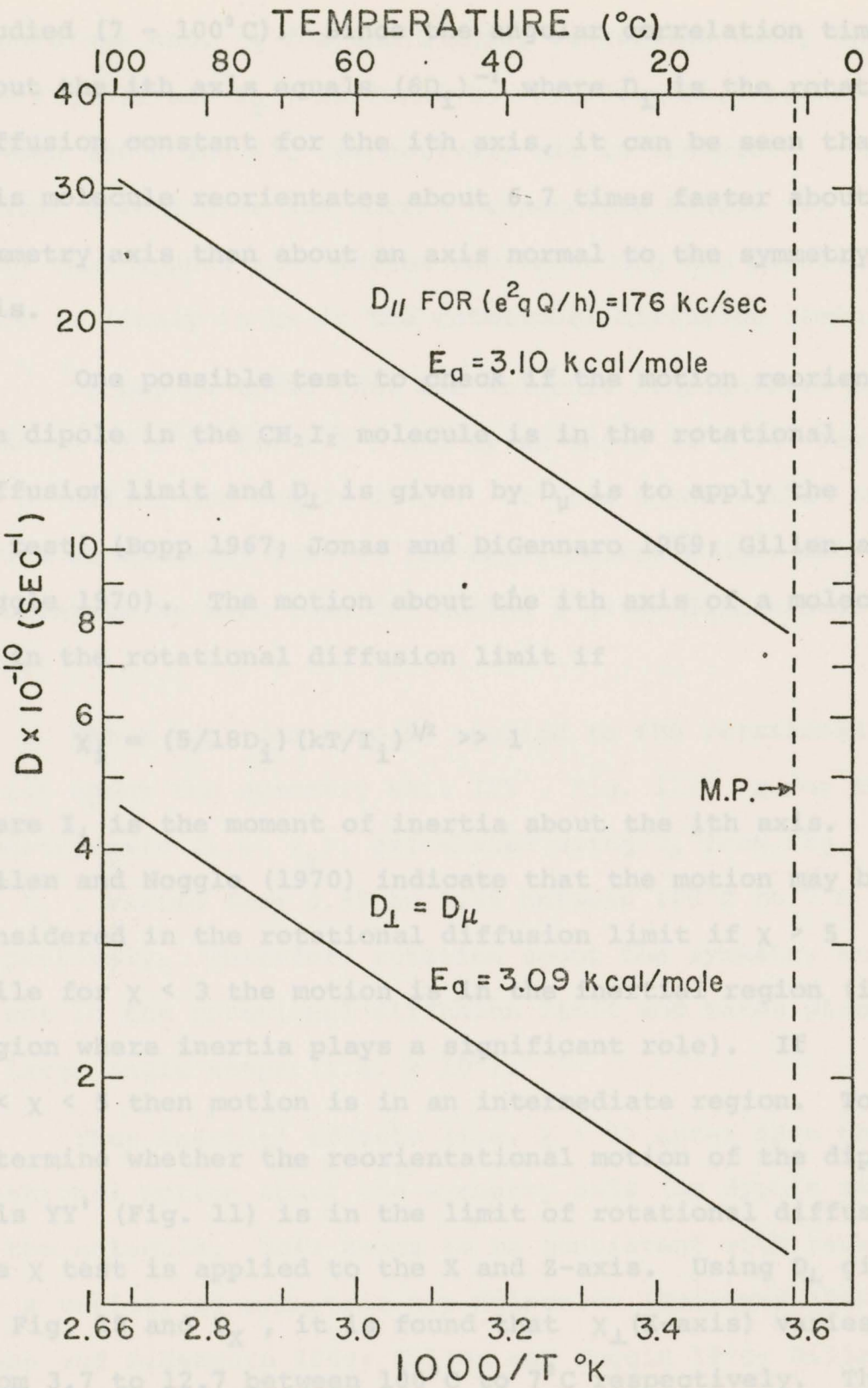

Fig. 18 Plots of $\ln D_{\perp}$ and $\ln D_{//}$ versus $1000/T^{0}K$

studied (7 - 100°C). Since the angular correlation time about the ith axis equals $(6D_i)^{-1}$ where D_i is the rotational diffusion constant for the ith axis, it can be seen that this molecule reorientates about 6.7 times faster about the symmetry axis than about an axis normal to the symmetry axis.

One possible test to check if the motion reorientating the dipole in the CH_2I_2 molecule is in the rotational diffusion limit and $D_\perp$ is given by D_μ is to apply the 'χ test' (Bopp 1967; Jonas and DiGennaro 1969; Gillen and Noggle 1970). The motion about the ith axis of a molecule is in the rotational diffusion limit if

$$\chi_i = (5/18D_i)(kT/I_i)^{1/2} >> 1$$

where I_i is the moment of inertia about the ith axis. Gillen and Noggle (1970) indicate that the motion may be considered in the rotational diffusion limit if $\chi > 5$ while for $\chi < 3$ the motion is in the inertial region (i.e. region where inertia plays a significant role). If $3 < \chi < 5$ then motion is in an intermediate region. To determine whether the reorientational motion of the dipole axis YY' (Fig. 11) is in the limit of rotational diffusion, the χ test is applied to the X and Z-axis. Using $D_\perp$ given in Fig. 18 and I_X, it is found that $\chi_\perp$(X-axis) varies from 3.7 to 12.7 between 100°C to 7°C respectively. This indicates that $\chi_\perp$(X-axis) is greater than 5 for most of the temperature range studied (7 - 100°C) except the high

temperature end. χ for the Z-axis, calculated using $D_\perp$ from Fig. 18 and I_Z , is found to vary from 22.4 to 76 between 100°C and 7°C respectively and is therefore greater than 5 over the entire temperature range. It would thus appear that motion reorientating the dipole in CH_2I_2 is likely to be in the rotational diffusion limit.

It may be noted that the molecule reorientates by an angle of $\lesssim 5^0$ for $\chi \gtrsim 5$ and by an angle of $\gtrsim 10^0$ for $\chi \lesssim 3$ (Gillen and Noggle 1970). It thus appears that the dipole or symmetry axis of the CH_2I_2 molecule does not reorientate by more than 10^0 during a given diffusional step.

The χ test can also be applied to the rotational motion about the symmetry axis (YY', Fig. 11). χ for the symmetry axis (i.e. $\chi_{//}$), calculated using $D_{//}$ from Fig. 18 and I_Y , varies from 0.55 to 1.85 between 100°C to 7°C respectively. Therefore rotation about the symmetry axis is not in the rotational diffusion limit and takes place by large angle steps (i.e. $> 10^0$).

Thus inertial effects (i.e. $\chi < 3$) enter into the rotational motion about the symmetry axis (or dipole axis) of the molecule. This seems to be consistent with results for a variety of symmetric top molecules (Huntress 1969; Jonas and DiGennaro 1969; Gillen and Noggle 1970; Gillen et al. 1971).

Another way of checking if $D_\perp$ is in the diffusion limit and D_μ can be used to give $D_\perp$ is to calculate the intramolecular dipole-dipole contribution to the relaxation and then compare the results with the experimental values. $(1/T_1)_{dd\text{-}intra}$ can be calculated using the approach outlined at the end of sec.(3.4). This involves the evaluation of $(1/T_1)_{dd\text{-}intra}$ using eq.(3.14), where $(\tau_c)_{dd}$ is replaced by correlation times that apply to the individual internuclear vectors.

Considering the jth nucleus to be a proton (H), and the kth nucleus to be an iodine (I) in eq.(3.14), $(1/T_1)_{dd\text{-}intra}$ for a CH_2I_2 molecule is given by

$$(1/T_1)_{dd\text{-}intra} = 2\hbar^2\gamma_H^4 I_H(I_H+1)r_{HH}^{-6}(\tau_c)_{HH} + (8/3)\hbar^2\gamma_H^2\gamma_I^2 I_I(I_I+1)r_{HI}^{-6}(\tau_c)_{HI} \qquad (4.17)$$

where the subscripts j and k have been replaced by H and I. $(\tau_c)_{HH}$ and $(\tau_c)_{HI}$ are the correlation times involved in the reorientation of the internuclear vectors H-H and H-I respectively. Using the values of r_{HH} = 1.785 Å and r_{HI} = 2.671 Å (Appendix B), $\hbar$ = 1.0545 x 10^{-27}erg-sec, and other constants given on page 57, eq.(4.17) can be written as

$$(1/T_1)_{dd\text{-}intra} = 2.64 \times 10^{10}(\tau_c)_{HH} + 0.147 \times 10^{10}(\tau_c)_{HI} \quad (4.18)$$

Replacing $(\tau_c)_{HH}$ and $(\tau_c)_{HI}$ by correlation times given by eq.(3.24), $(1/T_1)_{dd\text{-}intra}$ becomes the following

$$(1/T_1)_{dd\text{-}intra} = 2.64 \times 10^{10}\left[\frac{(1/4)(3\cos^2\theta_{HH} - 1)^2}{6D_\perp} + \frac{3\sin^2\theta_{HH}\cos^2\theta_{HH}}{5D_\perp + D_{//}} + \frac{(3/4)\sin^4\theta_{HH}}{2D_\perp + 4D_{//}}\right] + 0.147 \times 10^{10}\left[\frac{(1/4)(3\cos^2\theta_{HI} - 1)^2}{6D_\perp} + \frac{3\sin^2\theta_{HI}\cos^2\theta_{HI}}{5D_\perp + D_{//}} + \frac{(3/4)\sin^4\theta_{HI}}{2D_\perp + 4D_{//}}\right] \quad (4.19)$$

where θ_{HH} is the angle between the symmetry axis and the H-H internuclear vector,

θ_{HI} is the angle between the symmetry axis and the H-I internuclear vector.

It can be seen from Fig. 11 that $\theta_{HH} = 90^0$. By substituting $D_{//}$ and $D_\perp$ from Fig. 18 and the angles θ_{HH} and θ_{HI} (Appendix B, eq.B.7) into eq.(4.19), $(1/T_1)_{dd\text{-}intra}$ is

obtained. The solution of eq.(4.19) is given in Appendix A. Fig. 19 shows a plot of $\ln(1/T_1)_{dd\text{-}intra}$ versus $1000/T^0K$ for $(e^2qQ/h)_D$ = 176 kc/sec. The plot is a straight line with an activation energy of 3.10 kcal/mole. It can be seen from Fig. 19 that the calculated values of $(1/T_1)_{dd\text{-}intra}$ agree very well with the experimental values of $(1/T_1)_{dd\text{-}intra}$. This would indicate that the assumption $D_\mu = D_\perp$ is valid for this liquid and the rotational motion can be adequately described by the microviscosity theory for rotational diffusion.

The contributions due to interactions between identical spins and between nonidentical spins can also be obtained from eq.(4.18). The results show that the contribution due to identical spins is 95% of $(1/T_1)_{dd\text{-}intra}$ and the contribution due to nonidentical spins is 5% of $(1/T_1)_{dd\text{-}intra}$.

4.7 $(1/T_1)_{dd\text{-}inter}$ Results

The experimental values of $(1/T_1)_{dd\text{-}inter}$ can also be compared to values predicted from the Bloembergen, Purcell and Pound (BPP) theory (eq.3.17). The macroscopic viscosity η in the Stokes-Einstein relation (eq.3.18) is modified by Gierer and Wirtz (1953) by introducing a translational microviscosity factor f_t. This leads to the following expression for the coefficient of self-diffusion, D,

$$D = kT/6\pi\eta a f_t \quad .$$

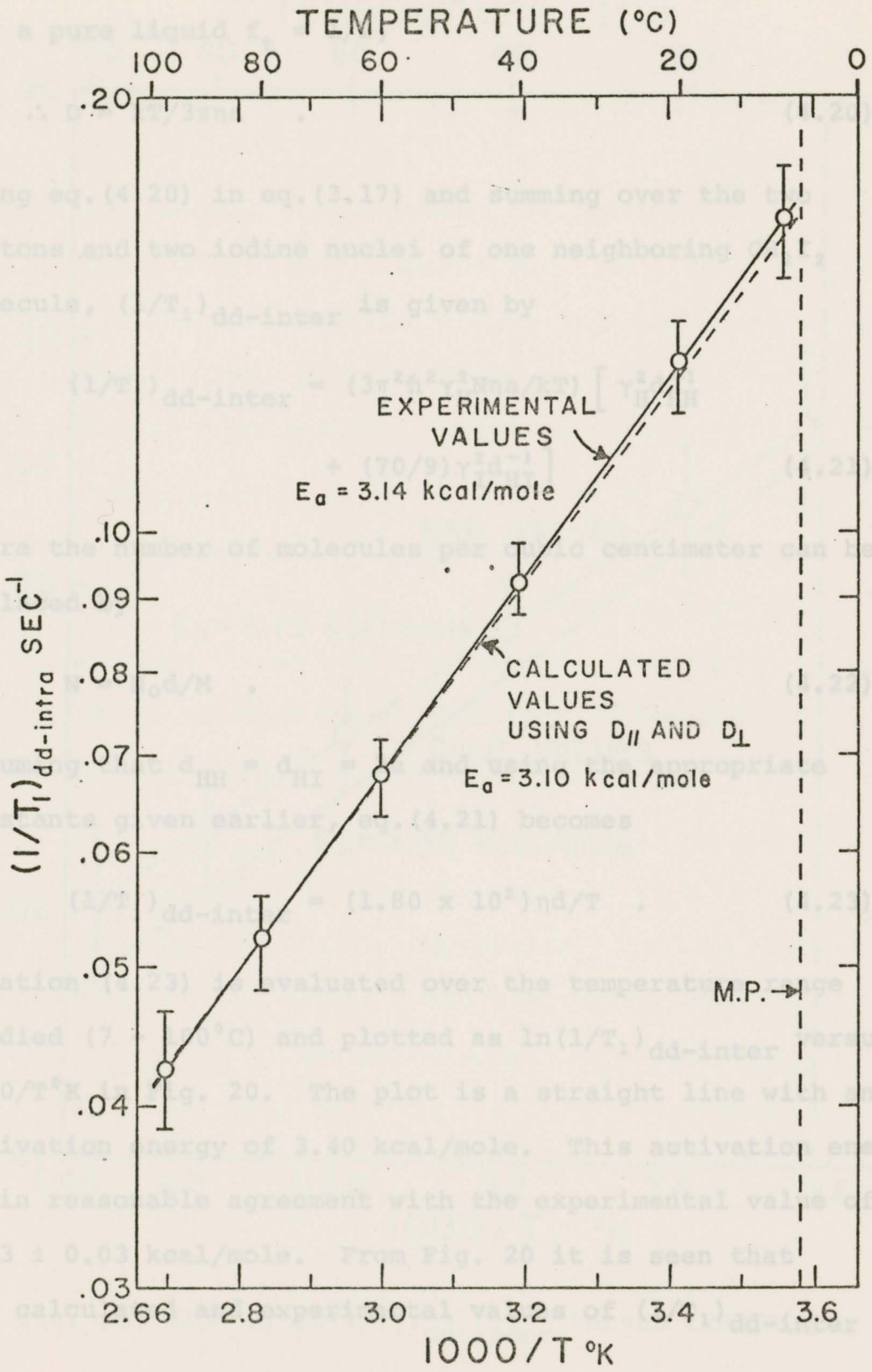

Fig. 19 Plots of experimental $(1/T_1)_{dd\text{-}intra}$ and $(1/T_1)_{dd\text{-}intra}$ calculated using $D_{\perp}$ and D_{II} versus $1000/T^0K$

For a pure liquid $f_t = 1/2$,

$$\therefore D = kT/3\pi\eta a \quad . \tag{4.20}$$

Using eq.(4.20) in eq.(3.17) and summing over the two protons and two iodine nuclei of one neighboring CH_2I_2 molecule, $(1/T_1)_{dd\text{-inter}}$ is given by

$$(1/T_1)_{dd\text{-inter}} = (3\pi^2\hbar^2\gamma_H^2 N\eta a/kT)\left[\gamma_H^2 d_{HH}^{-1} + (70/9)\gamma_I^2 d_{HI}^{-1}\right] \tag{4.21}$$

where the number of molecules per cubic centimeter can be replaced by

$$N = N_o d/M \quad . \tag{4.22}$$

Assuming that $d_{HH} = d_{HI} = 2a$ and using the appropriate constants given earlier, eq.(4.21) becomes

$$(1/T_1)_{dd\text{-inter}} = (1.80 \times 10^2)\eta d/T \quad . \tag{4.23}$$

Equation (4.23) is evaluated over the temperature range studied (7 - 100°C) and plotted as $\ln(1/T_1)_{dd\text{-inter}}$ versus $1000/T^0K$ in Fig. 20. The plot is a straight line with an activation energy of 3.40 kcal/mole. This activation energy is in reasonable agreement with the experimental value of 3.13 ± 0.03 kcal/mole. From Fig. 20 it is seen that the calculated and experimental values of $(1/T_1)_{dd\text{-inter}}$

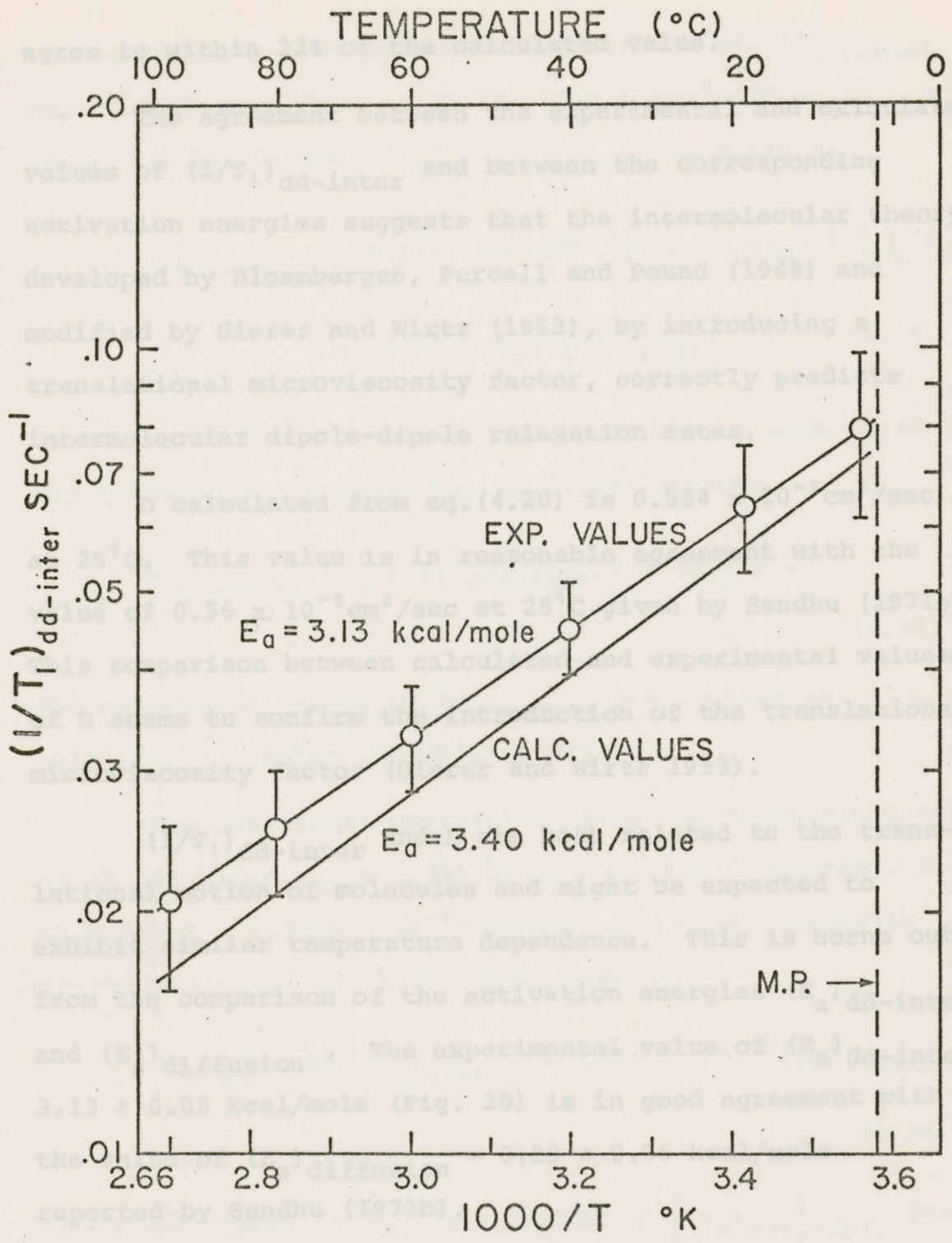

Fig. 20 Plot of $\ln(1/T_1)_{dd\text{-}inter}$ versus $1000/T^0K$

agree to within 22% of the calculated value.

The agreement between the experimental and calculated values of $(1/T_1)_{dd\text{-}inter}$ and between the corresponding activation energies suggests that the intermolecular theory developed by Bloembergen, Purcell and Pound (1948) and modified by Gierer and Wirtz (1953), by introducing a translational microviscosity factor, correctly predicts intermolecular dipole-dipole relaxation rates.

D calculated from eq.(4.20) is $0.584 \times 10^{-5} cm^2/sec$ at 25^0C. This value is in reasonable agreement with the value of $0.56 \times 10^{-5} cm^2/sec$ at 25^0C given by Sandhu (1971b). This comparison between calculated and experimental values of D seems to confirm the introduction of the translational microviscosity factor (Gierer and Wirtz 1953).

$(1/T_1)_{dd\text{-}inter}$ and D are both related to the translational motion of molecules and might be expected to exhibit similar temperature dependence. This is borne out from the comparison of the activation energies $(E_a)_{dd\text{-}inter}$ and $(E_a)_{diffusion}$. The experimental value of $(E_a)_{dd\text{-}inter} = 3.13 \pm 0.03$ kcal/mole (Fig. 20) is in good agreement with the value of $(E_a)_{diffusion} = 3.29 \pm 0.06$ kcal/mole reported by Sandhu (1971b).

4.8 Rotational and Translational Correlation Times

Using the experimental values of $(1/T_1)_{dd\text{-}inter}$,

the correlation time for translational motion, $(\tau_c)_{transl}$, can be evaluated from eq.(3.16) with r replaced by a. Using eqs.(3.16) and (3.17), $(\tau_c)_{transl}$ is given by

$$(\tau_c)_{transl} = (a^2/12)(\pi\hbar^2\gamma_H^2 N)^{-1}\left[(2/3)I_H(I_H+1)\gamma_H^2\sum_H d_{HH}^{-1} + (4/9)\sum_I I_I(I_I+1)\gamma_I^2 d_{HI}^{-1}\right] . \quad (4.24)$$

Substituting the value of N from eq.(4.22), a from eq.(4.14) and assuming $d_{HH} = d_{HI} = 2a$, eq.(4.24) becomes

$$(\tau_c)_{transl} = \left[(1/T_1)_{dd\text{-}inter}/4.028d^2\right] \times 10^{-8} . \quad (4.25)$$

The calculated values of $(\tau_c)_{transl}$ are plotted as $\ln(\tau_c)_{transl}$ versus $1000/T^0K$ in Fig. 21.

The rotational correlation time can be obtained from eq.(3.14) using $r_{HH} = 1.785$ Å, $r_{HI} = 2.671$ Å (Appendix B, eq.B.5), $\hbar = 1.0545 \times 10^{-27}$ erg-sec, and other constants previously given (p. 57). This leads to

$$(\tau_c)_{dd} = \left[(\tau_c)_{rot}\right]_{expt.} = 3.559 \times 10^{-11}(1/T_1)_{dd\text{-}intra} \quad (4.26)$$

where the symbol $(\tau_c)_{dd}$ is replaced by $\left[(\tau_c)_{rot}\right]_{expt.}$ for convenience. $\left[(\tau_c)_{rot}\right]_{expt.}$ is evaluated from eq.(4.26) using the experimental values of $(1/T_1)_{dd\text{-}intra}$ shown in

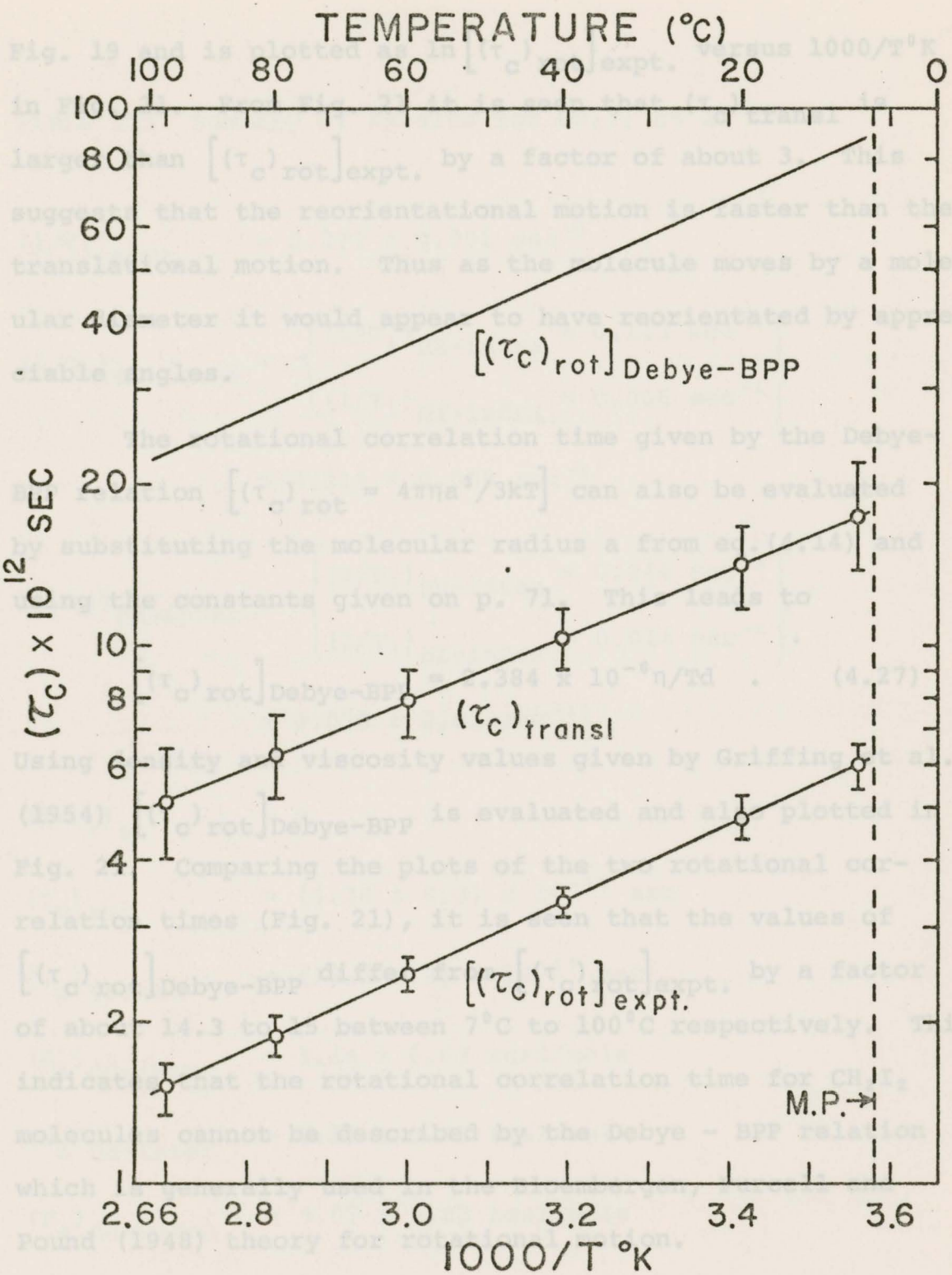

Fig. 21 Plots of $\ln(\tau_c)_{transl}$, $\ln[(\tau_c)_{rot}]_{expt.}$ and $\ln[(\tau_c)_{rot}]_{Debye-BPP}$ versus $1000/T^0K$

Fig. 19 and is plotted as $\ln\left[(\tau_c)_{rot}\right]_{expt.}$ versus $1000/T^0K$ in Fig. 21. From Fig. 21 it is seen that $(\tau_c)_{transl}$ is larger than $\left[(\tau_c)_{rot}\right]_{expt.}$ by a factor of about 3. This suggests that the reorientational motion is faster than the translational motion. Thus as the molecule moves by a molecular diameter it would appear to have reorientated by appreciable angles.

The rotational correlation time given by the Debye-BPP relation $\left[(\tau_c)_{rot} = 4\pi\eta a^3/3kT\right]$ can also be evaluated by substituting the molecular radius a from eq.(4.14) and using the constants given on p. 71. This leads to

$$\left[(\tau_c)_{rot}\right]_{Debye-BPP} = 2.384 \times 10^{-6}\eta/Td \quad . \qquad (4.27)$$

Using density and viscosity values given by Griffing et al. (1954) $\left[(\tau_c)_{rot}\right]_{Debye-BPP}$ is evaluated and also plotted in Fig. 21. Comparing the plots of the two rotational correlation times (Fig. 21), it is seen that the values of $\left[(\tau_c)_{rot}\right]_{Debye-BPP}$ differ from $\left[(\tau_c)_{rot}\right]_{expt.}$ by a factor of about 14.3 to 15 between 7^0C to 100^0C respectively. This indicates that the rotational correlation time for CH_2I_2 molecules cannot be described by the Debye - BPP relation which is generally used in the Bloembergen, Purcell and Pound (1948) theory for rotational motion.

The results for CH_2I_2 at 25^0C are summarized in Table III.

TABLE III Summary of Results for CH_2I_2 at 25°C

$(1/T_1)_{expt.} = 0.177 \pm 0.002 \text{ sec}^{-1}$

$$(1/T_1)_{dd\text{-}intra} = \left\{ \begin{array}{l} (1/T_1)_{HH\text{-}intra} = 0.113 \text{ sec}^{-1} \\ (1/T_1)_{HI\text{-}intra} = 0.006 \text{ sec}^{-1} \end{array} \right\}$$

$$= 0.119 \pm 0.008 \text{ sec}^{-1}$$

$$(1/T_1)_{dd\text{-}inter} = \left\{ \begin{array}{l} (1/T_1)_{HH\text{-}inter} = 0.044 \text{ sec}^{-1} \\ (1/T_1)_{HI\text{-}inter} = 0.014 \text{ sec}^{-1} \end{array} \right\}.$$

$$= 0.058 \pm 0.01 \text{ sec}^{-1}$$

$(1/T_1)_{sr} = 0$

$(\tau_c)_{rot} = (4.30 \pm 0.3) \times 10^{-12} \text{ sec}$

$(\tau_c)_{transl} = (13.1 \pm 2) \times 10^{-12} \text{ sec}$

$(E_a)_{dd\text{-}intra} = 3.14 \pm 0.03 \text{ kcal/mole}$

$(E_a)_{dd\text{-}inter} = 3.13 \pm 0.03 \text{ kcal/mole}$

$(E_a)_{deuteron} = 3.07 \pm 0.02 \text{ kcal/mole}$

CHAPTER 5

SUMMARY AND CONCLUSIONS

In this thesis a study of the nuclear spin-lattice relaxation in CH_2I_2 - CD_2I_2 mixtures and CD_2I_2 has been described in order to separate the various mechanisms contributing to relaxation and gain some information about molecular motions of the CH_2I_2 molecule.

Results of the study of T_1 of protons in mixtures of CH_2I_2 - CD_2I_2 as a function of concentration and T_1 of deuterons in CD_2I_2 between 7 - 100°C are summarized below:

1) The intramolecular dipole-dipole and the intermolecular dipole-dipole contributions are temperature dependent and are found to be 67.5% and 32.5% of the total relaxation respectively over the temperature range studied (7 - 100°C). The intra- and intermolecular dipole-dipole contributions due to interactions between nonidentical spins are 5% of $(1/T_1)_{dd\text{-}intra}$ and 24% of $(1/T_1)_{dd\text{-}inter}$ respectively.

2) The spin-rotational contribution is zero over the temperature range studied.

3) The activation energies of the intermolecular

dipole-dipole and intramolecular dipole-dipole contributions are 3.13 ± 0.03 kcal/mole and 3.14 ± 0.03 kcal/mole respectively. The activation energy obtained from the deuteron T_1 data is 3.07 ± 0.02 kcal/mole.

4) The rotational motion may be adequately described by microviscosity theory for rotational diffusion.

5) The rotational motion of this molecule is anisotropic. Reorientation about the symmetry axis occurs faster than the reorientation of the symmetry axis.

6) A comparison between the correlation times of rotational and translational motion shows that it takes about 3 times as long for the molecule to move by a distance of the order of a molecular diameter than to reorientate through a radian.

7) The experimental values of the rotational correlation time do not agree with the values predicted by the Debye - BPP expression $(4\pi\eta a^3/3kT)$.

8) The experimental values of the intermolecular dipole-dipole contribution agree to within 22% of the values predicted by the BPP

theory modified by Gierer and Wirtz (1953) to include the translational microviscosity factor.

It may be useful to extend this work as follows:

1) Since the boiling point of CH_2I_2 is about 180°C, it would be of interest to measure T_1 in mixtures as a function of concentration between 100 - 180°C to check if spin-rotational contribution is present in that temperature range. However, this would require some changes in the temperature control system.

2) A study of T_1 in other similar liquids such as CH_2Br_2 may help to confirm results found in this work and also provide more information about molecular motions of this type of molecule.

3) A knowledge of the quadrupole coupling constant for the deuteron in CD_2I_2 would be extremely helpful in confirming these results.

4) It would be useful to extend the measurements of T_1 in solid CH_2I_2 to obtain some information about the solid state properties of CH_2I_2.

REFERENCES

Abragam, A. 1961. The Principles of Nuclear Magnetism. Oxford University Press, London.

Andrew, E.R. 1955. Nuclear Magnetic Resonance. Cambridge University Press, London.

Blicharski, J., Hennel, J.W., Krynicki, K., Mikulski, J., Waluga, T., Zapalski, G. 1960. Temperature dependence of proton spin-lattice relaxation times in some pure liquids. Arch. Sci. (Geneva) 13, 452.

Bloch, F. 1946. Nuclear induction. Phys. Rev. 70, 460.

Bloch, F., Hansen, W.W., Packard, M. 1946. Nuclear induction. Phys. Rev. 69, 127.

Bloch, F. and Siegert, A. 1940. Magnetic resonance for nonrotating fields. Phys. Rev. 57, 522.

Bloembergen, N., Purcell, E.M., Pound, R.V. 1948. Relaxation effects in nuclear magnetic resonance absorption. Phys. Rev. 73, 679.

Bonera, G. and Rigamonti, A. 1965a. Intra- and Intermolecular contributions to the proton spin-lattice relaxation in liquids. J. Chem. Phys. 42, 171.

Bonera, G. and Rigamonti, A. 1965b. Electric-field gradients in liquids by deuteron quadrupole relaxation. J. Chem. Phys. 42, 175.

Bopp, T.T. 1967. Magnetic resonance studies of anisotropic molecular rotation in liquid acetonitrile-d_3. J. Chem. Phys. 47, 3621.

de Wit, G.A. 1966. Nuclear spin-lattice relaxation in solid methane at low temperatures. Ph. D. Thesis, The University of British Columbia, British Columbia.

Gierer, A. and Wirtz, K. 1953. Molekulare theorie der mikroreibung. Z. Naturf. A 8, 532.

Gillen, K.T. and Noggle, J.H. 1970. NMR studies of the rotational diffusion of symmetric top molecules in liquids. J. Chem. Phys. 53, 801.

Gillen, K.T., Schwartz, M., Noggle, J.H. 1971. N.M.R. relaxation time studies in liquid methyl iodide. Mol. Phys. 20, 899.

Gray, K.W., Hardy, W.N., Noble, J.D. 1966. Optimized pulsed NMR single coil circuit design. Rev. Sci. Instr. 37, 587.

Griffing, V., Cargyle, M.A., Corvese, L., Eby, D. 1954. Temperature coefficients of viscosity of some halogen substituted organic compounds. J. Phys. Chem. 58, 1054.

Hahn, E.L. 1950. Spin echoes. Phys. Rev. 80, 580.

Hassel, O. and Viervoll, H. 1947. Electron diffraction investigation of molecular structure. Acta Chem. Scand. 1, 149.

Herzberg, G. 1945. Molecular Spectra and Molecular Structure. II. Infrared and Raman Spectra of Polyatomic Molecules. D. Van Nostrand Company, Inc., Princeton.

Hubbard, P.S. 1963. Theory of nuclear magnetic relaxation by spin-rotational interactions in liquids. Phys. Rev. 131, 1155.

Huntress, Jr., W.T. 1968. Effects of anisotropic molecular rotational diffusion on nuclear magnetic relaxation in liquids. J. Chem. Phys. 48, 3524.

Huntress, Jr., W.T. 1969. A nuclear magnetic resonance study of anisotropic molecular rotation in liquid chloroform and in chloroform-benzene solution. J. Phys. Chem. 73, 103.

Jonas, J. and DiGennaro, T.M. 1969. Anisotropic molecular reorientation in methyl-d_3-acetylene in the liquid state. J. Chem. Phys. 50, 2392.

Kubo, R. and Tomita, K. 1954. A general theory of magnetic resonance absorption. J. Phys. Soc. Japan 9, 888.

Kukolich, S.G., Nelson, A.C., Ruben, D.J. 1971. Molecular beam measurement of hyperfine structure of fluoroform. J. Mol. Spectry. 40, 33.

Lees, J., Muller, B.H., Noble, J.D. 1961. Degassing of liquids for nuclear spin-lattice relaxation studies. J. Chem. Phys. 34, 341.

Millett, F.S. and Dailey, B.P. 1972. NMR determination of some deuterium quadrupole coupling constants in nematic solutions. J. Chem. Phys. 56, 3249.

Mitchell, R.W. and Eisner, M. 1960. Nuclear spin-lattice relaxation in solutions. J. Chem. Phys. 33, 86.

Nederbragt, G.W. and Reilly, C.A. 1956. Nuclear spin-lattice relaxation times of aromatic and aliphatic protons. J. Chem. Phys. 24, 1110.

Nolle, A.W. and Mahendroo, P.P. 1960. Effects of pressure on proton spin-lattice relaxation in several degassed organic liquids. J. Chem. Phys. 33, 863.

Pound, R.V. 1950. Nuclear electric quadrupole interactions in crystals. Phys. Rev. 79, 685.

Powles, J.G. and Figgins, R. 1966. Molecular motion in liquid benzene by nuclear magnetic resonance. Mol. Phys. 10, 155.

Powles, J.G. and Figgins, R. 1967. Molecular motion in liquid bromobenzene and 1, 3, 5 trideuterobenzene by nuclear magnetic resonance. Mol. Phys. 13, 253.

Powles, J.G., Rhodes, M., Strange, J.H. 1966. Deuteron spin-lattice relaxation in benzene, bromobenzene, water and ammonia. Mol. Phys. 11, 515.

Prichard, W.H. and Orville-Thomas, W.J. 1963. Infra-red dispersion studies. Trans. Faraday Soc. 59, 2218.

Purcell, E.M., Torrey, H.C., Pound, R.V. 1946. Resonance absorption by nuclear magnetic moments in a solid. Phys. Rev. 69, 37.

Ragle, J.L. and Sherk, K.L. 1969. Deuteron quadrupole coupling in some solid chlorinated hydrocarbons. J. Chem. Phys. 50, 3553.

Redfield, A.G. 1957. On the theory of relaxation processes. IBM J. Res. Develop. 1, 19.

Robinson, H., Dehmelt, H.G., Gordy, W. 1954. Nuclear quadrupole couplings in solid bromides and iodides. J. Chem. Phys. 22, 511.

Sandhu, H.S. 1964. Proton magnetic resonance in methane and its deuterated modifications. Ph. D. Thesis, The University of British Columbia, British Columbia.

Sandhu, H.S. 1966. Effect of paramagnetic impurities on proton spin-lattice relaxation time in methane. J. Chem. Phys. 44, 2320.

Sandhu, H.S. 1969. Nuclear spin-lattice relaxation in some pure liquids. J. Chem. Phys. 51, 2452.

Sandhu, H.S. 1971a. Use of a gettering material to obtain oxygen-free liquid samples for nuclear spin relaxation studies. Can. J. Chem. 49, 1008.

Sandhu, H.S. 1971b. Self-diffusion measurements in pure liquids using spin echoes. Can. J. Phys. 49, 1069.

Sandhu, H.S., Lees, J., Bloom, M. 1960. Removal of oxygen from methane and the use of nuclear spin relaxation to measure oxygen concentration. Can. J. Chem. 38, 493.

Shimizu, H. 1964. Effect of molecular shape on nuclear magnetic relaxation. II. Quadrupole relaxation. J. Chem. Phys. 40, 754.

Smith, D.W.G. and Powles, J.G. 1966. Proton spin-lattice relaxation in liquid water and liquid ammonia. Mol. Phys. 10, 451.

Thaddeus, P., Krisher, L.C., Loubser, J.H.N. 1964. Hyperfine structure in the microwave spectrum of HDO, HDS, CH_2O and CHDO: Beam-Maser spectroscopy on asymmetric-top molecules. J. Chem. Phys. 40, 257.

Wallman, H., MacNee, A.B., Gadsden, C.P. 1948. A low-noise amplifier. Proc. I.R.E. 36, 700.

Wangsness, R.K. and Bloch, F. 1953. The dynamic theory of nuclear induction. Phys. Rev. 89, 728.

Woessner, D.E. 1962. Nuclear spin relaxation in ellipsoids undergoing rotational Brownian motion. J. Chem. Phys. 37, 647.

Woessner, D.E., Snowden, Jr., B.S., Strom, E.T. 1968. A study of molecular reorientation in liquid acetonitrile by nuclear spin-lattice relaxation. Mol. Phys. 14, 265.

Wofsy, S.C., Muenter, J.S., Klemperer, W. 1970. Hyperfine structure and dipole moment of CH_3D. J. Chem. Phys. 53, 4005.

APPENDIX A

COMPUTER PROGRAM LISTING

Program I evaluates the least squares lines for the mixtures and separates the intermolecular dipole-dipole contribution from the intramolecular contribution. The input consists of the experimental T_1's and the corresponding temperatures.

Program II A calculates $D_{//}$ from the following equation which was obtained by solving eq.(3.25) for $D_{//}$ and taking I = 1

$$D_{//} = \frac{-b \pm (b^2-4ac)^{1/2}}{2a}$$

where $a = 24D_{\perp}(\tau_c)_q - 4A$,

$b = 132D_{\perp}^2(\tau_c)_q - (22A + 24B + 6C)D_{\perp}$,

$c = 60D_{\perp}^3(\tau_c)_q - (10A + 12B + 30C)D_{\perp}^2$,

$A = (1/4)(3\cos^2\theta - 1)^2$,

$B = 3\sin^2\theta\cos^2\theta$,

$C = (3/4)\sin^4\theta$,

$(\tau_c)_q = (2/3\pi^2)(e^2qQ/h)^{-2}(1/T_1)_q$.

The input data consists of values of $D_{\perp}$, together with the

corresponding temperatures and values of $(1/T_1)_q$.

Program II B evaluates $(1/T_1)_{dd\text{-}intra}$ using eq.(4.19).

The output of Program II gives the following calculated values: $D_{//}$, $(\tau_c)_{HH}$, $(\tau_c)_{HI}$, $(\tau_c)_q$, $(1/T_1)_{HH\text{-}intra}$, $(1/T_1)_{HI\text{-}intra}$ and $(1/T_1)_{dd\text{-}intra}$.

```
C      PROGRAM I - CALCULATION OF LEAST SQUARES LINES AND SEPERATION OF
C                  INTERMOLECULAR DIPOLE - DIPOLE AND INTRAMOLECULAR
C                  CONTRIBUTIONS.
C
C
C
      DIMENSION A(9),B(9),C(9),D(9),E(9),T(4),XR(4),AH(9),BA(9),INTRA(9)
     2,INTER(9),DITRA(9),DITER(9),X3(9),X5(9),ONTRA(9),ONTER(9),BONAR(9)
     2,BONER(9),BONTRA(9),BONTER(9),DEVA(9),DEVB(9),CUT(9),FUT(9),WAL(9)
     2,WUL(9),XH(9)
      INTEGER COUNT,CON
      REAL INTRA,INTER
      CON=0
  999 CON=CON+1
      M=0
      COUNT=0
      SUMX=0
      SUMY=0
      SUMXY=0
      SUMXSQ=0
      READ(5,101)N
  101 FORMAT(3X,I3)
      WRITE(6,201)N
  201 FORMAT('-',6X,'N=',I3)
      WRITE(6,111)
  111 FORMAT('-',2X,'T',6X,'X=1000/T',6X,'T1',9X,'1/T1',7X,'Y=LNT1',10X,
     2'T',6X,'X=1000/T',6X,'T1',9X,'1/T1',7X,'Y=LNT1')
   33 READ(5,301)XX3,YY1
  301 FORMAT(F8.4,2X,F8.4)
      XX1=XX3+273.16
      X=1000/XX1
      YY2=1/YY1
      Y=ALOG(YY1)
      M=M+1
      GO TO(34,35),M
   34 WRITE(6,401)XX3,X,YY1,YY2,Y
  401 FORMAT(' ',F6.2,4X,F6.4,6X,F5.2,6X,F6.4,6X,F6.4)
      GO TO 17
   35 WRITE(6,402)XX3,X,YY1,YY2,Y
  402 FORMAT('+',59X,F6.2,4X,F6.4,6X,F5.2,6X,F6.4,6X,F6.4)
      M=0
   17 CONTINUE
      COUNT=COUNT+1
      SUMX=SUMX+X
      SUMY=SUMY+Y
      SUMXY=SUMXY+(X*Y)
      SUMXSQ=SUMXSQ+X**2
      IF(COUNT.LT.N)GO TO 33
      DENOM=N*SUMXSQ-SUMX**2
      Z=(SUMY*SUMXSQ-SUMXY*SUMX)/DENOM
      Q=(N*SUMXY-SUMX*SUMY)/DENOM
      WRITE(6,501)SUMX,SUMY,SUMXY,SUMXSQ
  501 FORMAT('-',2X,'SUMX=',F8.3,2X,'SUMY=',F8.3,2X,'SUMXY=',F8.3,2X,'SU
     7MXSQ=',F8.3)
      WRITE(6,601)Z,Q
  601 FORMAT('-',10X,'A=',F8.4,6X,'B=',F8.4)
```

```
0046        WRITE(6,701)Z,Q
0047    701 FORMAT('-','THE LEAST SQUARES REGRESSION LINE IS Y = ',F8.4,F8.4,'
           2X')
0048        WRITE(6,801)
0049    801 FORMAT('-',9X,'X',9X,'Y',9X,'EXPY',9X,'INV. EXPY')
0050        XH1=2.7
0051        DO 19 J=1,9
0052        XH(J)=XH1
0053        XH1=XH1+0.1
0054     19 CONTINUE
0055        DO 2 J=1,9
0056        Y1=Z+Q*XH(J)
0057        YEXP=EXP(Y1)
0058        YINV=1/YEXP
0059        WRITE(6,901)XH(J),Y1,YEXP,YINV
0060    901 FORMAT(' ',6X,F8.4,2X,F8.4,3X,F8.4,7X,F8.5)
0061        A(J)=YINV
0062      2 CONTINUE
0063        GO TO(13,14,15,16),CON
0064     13 DO 3 J=1,9
0065        B(J)=A(J)
0066      3 CONTINUE
0067        GO TO 999
0068     14 DO 4 J=1,9
0069        C(J)=A(J)
0070      4 CONTINUE
0071        GO TO 999
0072     15 DO 5 J=1,9
0073        D(J)=A(J)
0074      5 CONTINUE
0075        GO TO 999
0076     16 DO 6 J=1,9
0077        E(J)=A(J)
0078      6 CONTINUE
      C
      C
0079        P=4
0080        WRITE(6,2222)
0081   2222 FORMAT('-','1000/T',4X,'INTERCEPTS FROM PLOTS OF 1/T1 VS. C',4X,'1
           2000/T',4X,'SLOPES FROM PLOTS OF 1/T1 VS. C')
0082        DO 303 J=1,9
0083        SUK=0
0084        SUY=0
0085        SUKY=0
0086        SUKSQ=0
0087        T(1)=B(J)
0088        T(2)=C(J)
0089        T(3)=D(J)
0090        T(4)=E(J)
0091        XR(1)=23.0/24.0
0092        XR(2)=18.4/24.0
0093        XR(3)=13.8/24.0
0094        XR(4)=9.2/24.0
0095        DO 202 I=1,4
0096        SUK=SUK+XR(I)
0097        SUY=SUY+T(I)
0098        SUKY=SUKY+(XR(I)*T(I))
0099        SUKSQ=SUKSQ+XR(I)**2
```

```
0100    202 CONTINUE
0101        DEMON=P*SUKSQ-(SUK**2)
0102        AH(J)=(SUY*SUKSQ-SUKY*SUK)/DEMON
0103        BA(J)=(P*SUKY-SUK*SUY)/DEMON
0104        SAKI=0
0105        DO 414 I=1,4
0106        SAKI=SAKI+(T(I)-(AH(J)+BA(J)*XR(I)))**2
0107    414 CONTINUE
0108        SAR=ABS((P-2)*((P*SUKSQ)-((SUK)**2)))
0109        DEVA(J)=SQRT((SAKI*SUKSQ)/SAR)
0110        DEVB(J)=SQRT((P*SAKI)/SAR)
0111        WRITE(6,1111)XH(J),AH(J),DEVA(J),XH(J),BA(J),DEVB(J)
0112   1111 FORMAT(' ',F6.4,6X,F8.5,2X,'PLUS OR MINUS',2X,F8.5,5X,F6.4,3X,F8.5
          2,2X,'PLUS OR MINUS',2X,F8.5)
0113    303 CONTINUE
0114        WRITE(6,3333)
0115   3333 FORMAT('-','1000/T',9X,'INTRA TOTALS',22X,'1000/T',9X,'INTER TOTAL
          2S')
0116        DO 505 J=1,9
0117        TOTS=(BA(J)/24)+(BA(J)*0.311)
0118        INTRA(J)=AH(J)-TOTS
0119        INTER(J)=(BA(J)+(BA(J)*0.311))
0120        DITRA(J)=DEVA(J)+((1/24)+0.311)*DEVB(J)
0121        DITER(J)=DEVB(J)*(1.311)
0122        WRITE(6,1111)XH(J),INTRA(J),DITRA(J),XH(J),INTER(J),DITER(J)
0123    505 CONTINUE
0124        POT=9
0125        TUBX=0
0126        TUBY=0
0127        TUBXY=0
0128        TUBXSQ=0
0129        DO 606 J=1,9
0130        CUT(J)=1/INTRA(J)
0131        ONTRA(J)=ALOG(CUT(J))
0132        TUBX=TUBX+XH(J)
0133        TUBY=TUBY+ONTRA(J)
0134        TUBXY=TUBXY+(XH(J)*ONTRA(J))
0135        TUBXSQ=TUBXSQ+XH(J)**2
0136    606 CONTINUE
0137        DUMMY=POT*TUBXSQ-TUBX**2
0138        AARB=((TUBY*TUBXSQ)-(TUBXY*TUBX))/DUMMY
0139        BARB=((POT*TUBXY)-(TUBX*TUBY))/DUMMY
0140        SOKI=2.7
0141        DO 707 J=1,9
0142        X3(J)=SOKI
0143        SOKI=SOKI+0.1
0144    707 CONTINUE
0145        BOXA=0
0146        DO 808 J=1,9
0147        BOXA=BOXA+(ONTRA(J)-(AARB+(BARB*X3(J))))**2
0148    808 CONTINUE
0149        ARR=SQRT((POT*BOXA)/ABS((POT-2)*((POT*TUBXSQ)-((TUBX)**2))))
0150        WRITE(6,4444)AARB,BARB,ARR
0151   4444 FORMAT('-',6X,'THE EQUATION OF THE INTRA-LINE IS LNTI =',2X,F8.5,2
          2X,2X,F8.5,3X,'(PLUS OR MINUS',2X,F8.5,')',3X'1000/T')
0152        FUMX=0
0153        FUMY=0
0154        FUMXY=0
```

```
0155          FUMXSQ=0
0156          DO 909 J=1,9
0157          FUT(J)=1/INTER(J)
0158          ONTER(J)=ALOG(FUT(J))
0159          FUMX=FUMX+XH(J)
0160          FUMY=FUMY+ONTER(J)
0161          FUMXY=FUMXY+(XH(J)*ONTER(J))
0162          FUMXSQ=FUMXSQ+XH(J)**2
0163      909 CONTINUE
0164          FUMMY=POT*FUMXSQ-FUMX**2
0165          AARB1=((FUMY*FUMXSQ)-(FUMXY*FUMX))/FUMMY
0166          BARB1=((POT*FUMXY)-(FUMX*FUMY))/FUMMY
0167          FOXI=2.7
0168          DO 115 J=1,9
0169          X5(J)=FOXI
0170          FOXI=FOXI+0.1
0171      115 CONTINUE
0172          FOXA=0
0173          DO 225 J=1,9
0174          FOXA=FOXA+(ONTER(J)-(AARB1+(BARB1*X5(J))))**2
0175      225 CONTINUE
0176          ERR=SQRT((POT*FOXA)/ABS((POT-2)*((POT*FUMXSQ)-((FUMX)**2))))
0177          WRITE(6,5555)AARB1,BARB1,ERR
0178     5555 FORMAT('-',6X,'THE EQUATION OF THE INTER-LINE IS LNT1 =',2X,F8.5,2
            2X,2X,F8.5,3X,'(PLUS OR MINUS',2X,F8.5,')',3X,'1000/T')
0179          WRITE(6,440)
0180      440 FORMAT('-','1000/T',4X,'INTRA VALUES FROM INTRA LINE',4X,'1000/T',
            24X,'INTER VALUES FROM INTER LINE')
0181          DO 599 J=1,9
0182          BONAR(J)=AARB+BARB*XH(J)
0183          WAL(J)=EXP(BONAR(J))
0184          BONTRA(J)=1/WAL(J)
0185          BONER(J)=AARB1+BARB1*XH(J)
0186          WUL(J)=EXP(BONER(J))
0187          BONTER(J)=1/WUL(J)
0188          WRITE(6,550)XH(J),BONTRA(J),XH(J),BONTER(J)
0189      550 FORMAT(' ',F6.4,14X,F6.4,17X,F6.4,12X,F6.4)
0190      599 CONTINUE
0191          ANTS=BARB*1.987
0192          AANTS=BARB1*1.987
0193          ANTI=ARR*1.987
0194          AANTI=ERR*1.987
0195          WRITE(6,1222)ANTS,ANTI
0196     1222 FORMAT('-','THE ACTIVATION ENERGY OF THE INTRA LINE IS',2X,F8.5,2X
            2,'PLUS OR MINUS',F8.5)
0197          WRITE(6,1223)AANTS,AANTI
0198     1223 FORMAT('-','THE ACTIVATION ENERGY OF THE INTER LINE IS',2X,F8.5,2X
            2,'PLUS OR MINUS',F8.5)
0199          WRITE(6,594)
0200      594 FORMAT(//////////)
0201          END
```

```
      C      PROGRAM IIA - CALCULATION OF D-PARALLEL
      C
      C
0001          DIMENSION T1(20),DPER(20),TEMP(20),DP10(20),CORRQ(20),ANS(20),BNS(
             220),CNS(20),DPARP(20),DPARM(20),RES1(20),CORHH(20),CORHI(20),T1HH(
             220),T1HI(20),T1INT(20)
0002          DOUBLE PRECISION PI,DARSIN
0003          READ(5,11)N
0004       11 FORMAT(3X,I3)
0005          WRITE(6,22)N
0006       22 FORMAT('-',6X,I3)
0007          DO 1 J=1,N
0008          READ(5,33)T1(J)
0009       33 FORMAT(F8.4)
0010        1 CONTINUE
0011          DO 2 J=1,N
0012          READ(5,33)DPER(J)
0013          DP10(J)=(DPER(J))*(10.0**10.0)
0014        2 CONTINUE
0015          DO 3 J=1,N
0016          READ(5,33)TEMP(J)
0017        3 CONTINUE
0018          COUPC=176.0*(10.0**3.0)
0019          CONST=(2.0/3.0)*((7.0/22.0)**2.0)*(1.0/(COUPC**2.0))
0020          ANGDE=54.75
0021          ANGHH=90.0
0022          ANGHI=48.355
0023          PI=2.0D0*DARSIN(1.0D0)
0024          POT=PI/180.0
0025          BUS=ANGDE*POT
0026          BAS=ANGHH*POT
0027          BUSHI=ANGHI*POT
0028          OP=COS(BUS)
0029          OM=SIN(BUS)
0030          OQ=COS(BAS)
0031          OL=SIN(BAS)
0032          OG=COS(BUSHI)
0033          OLL=SIN(BUSHI)
0034          AQ=.25*((3*(COS(BUS))**2)-1.0)**2
0035          BQ=3*((SIN(BUS))**2)*((COS(BUS))**2)
0036          CQ=.75*((SIN(BUS))**4)
0037          AHH=.25*((3*(COS(BAS))**2)-1.0)**2
0038          BHH=3*((SIN(BAS))*2)*((COS(BAS))**2)
0039          CHH=.75*((SIN(BAS))**4)
0040          AHI=.25*((3*(COS(BUSHI))**2)-1.0)**2
0041          BHI=3*((SIN(BUSHI))**2)*((COS(BUSHI))**2)
0042          CHI=.75*((SIN(BUSHI))**4)
0043          AANY=4.0*AQ
0044          ABC1=(22.0*AQ)+(24.0*BQ)+(6.0*CQ)
0045          ABC2=(10.0*AQ)+(12.0*BQ)+(30.0*CQ)
0046          CONH=2.6403*(10.0**10.0)
0047          CONI=0.1466*(10.0**10.0)
0048          DO 007 J=1,N
0049          CORRQ(J)=CONST*(1.0/T1(J))
0050          ANS(J)=(24.0*DP10(J)*CORRQ(J))-AANY
0051          BNS(J)=(132.0*(DP10(J)**2.0)*CORRQ(J))-(ABC1*DP10(J))
```

```
0052        CNS(J)=(60.0*(DP10(J)**3.0)*CORRQ(J))-(ABC2*(DP10(J)**2.0))
0053        DPARM(J)=(-BNS(J)-(SQRT((BNS(J)**2)-4*ANS(J)*CNS(J))))/(2*ANS(J))
0054        DPARP(J)=(-BNS(J)+(SQRT((BNS(J)**2)-4*ANS(J)*CNS(J))))/(2*ANS(J))
0055        IF(DPARP(J).GT.0)GO TO 88
0056        RES1(J)=DPARM(J)
0057        GO TO 99
0058     88 RES1(J)=DPARP(J)
0059     99 CONTINUE
      C
      C
      C     PROGRAM IIB - CALCULATION OF DD-INTRA FROM DEUTERON DATA
      C
      C
0060        CORHH(J)=(AHH/(6*DP10(J)))+(BHH/((5*DP10(J))+RES1(J)))+(CHH/((2*DP
           210(J))+4*RES1(J)))
0061        CORHI(J)=(AHI/(6*DP10(J)))+(BHI/((5*DP10(J))+RES1(J)))+(CHI/((2*DP
           210(J))+4*RES1(J)))
0062        T1HH(J)=COHH*CORHH(J)
0063        T1HI(J)=COHI*CORHI(J)
0064        T1INT(J)=T1HH(J)+T1HI(J)
0065     007 CONTINUE
0066        WRITE(6,999)
0067     999 FORMAT('-',' 1000/0K',5X,'T1',9X,'D PERP',9X,'D PARP',7X,'CORHH',9
           2X,'CORHI',9X,'1/T1HH',3X,'1/T1HI',3X,'1/T1INTRA DD',6X,'CORRQ')
0068        DO 77 J=1,N
0069        WRITE(6,888)TEMP(J),T1(J),DP10(J),RES1(J),CORHH(J),CORHI(J),T1HH(J
           2),T1HI(J),T1INT(J),CORRQ(J)
0070     888 FORMAT(' ',2X,F5.3,5X,F5.3,4X,E10.4,5X,E10.4,4X,E10.4,4X,E10.4,5X,
           2F7.5,2X,F7.5,6X,F7.5,7X,E10.4)
0071      77 CONTINUE
0072        END
```

APPENDIX B

CALCULATION OF THE DISTANCE BETWEEN PROTON AND IODINE NUCLEUS AND OF THE ANGLE BETWEEN H-I VECTOR AND SYMMETRY AXIS

Consider the co-ordinate system XYZ with its origin at O (center of mass) and a co-ordinate system X'Y'Z' with its origin O' coinciding with a proton (Fig. B.1) such that the corresponding axes of the two systems are parallel. By inspection of Fig. B.1 it is seen that

$$X_I' = (1/2)r_{HH}$$

$$Y_I' = r_1 + r_2 \qquad \text{(B.1)}$$

$$Z_I' = (1/2)r_{II} \quad .$$

Using the parameters in Table I and applying the cosine law, it can be easily shown that

$$r_{HH} = (2r_{HC}^2 - 2r_{HC}^2\cos\angle HCH)^{1/2} = 1.785 \text{ Å}$$

$$r_{II} = (2r_{IC}^2 - 2r_{IC}^2\cos\angle ICI)^{1/2} = 3.57 \text{ Å} \quad . \qquad \text{(B.2)}$$

From Fig. B.1 it is also seen that

$$r_1 = r_{HC}\cos\left[(1/2)\angle HCH\right] = 0.631 \text{ Å}$$

$$r_2 = r_{IC}\cos\left[(1/2)\angle ICI\right] = 1.144 \text{ Å} \quad . \qquad \text{(B.3)}$$

Substituting values from eq.(B.2) and (B.3) into eq.(B.1)

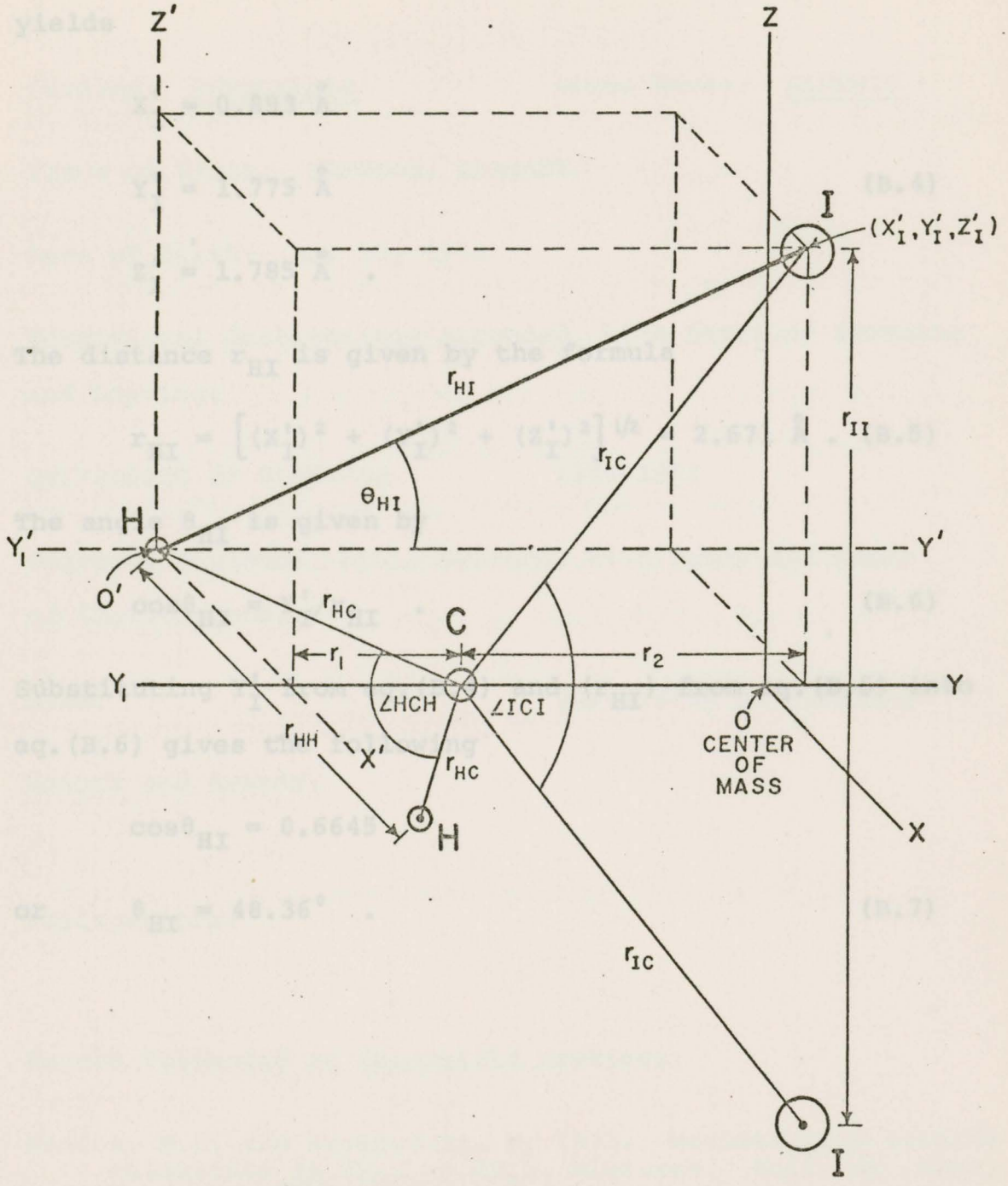

Fig. B.1 Diagram of CH_2I_2 molecule used in calculation of H-I distance and angle between H-I vector and symmetry axis

yields

$$X_I' = 0.893 \text{ Å}$$

$$Y_I' = 1.775 \text{ Å} \qquad \text{(B.4)}$$

$$Z_I' = 1.785 \text{ Å} \quad .$$

The distance r_{HI} is given by the formula

$$r_{HI} = \left[(X_I')^2 + (Y_I')^2 + (Z_I')^2\right]^{1/2} = 2.671 \text{ Å} \quad . \qquad \text{(B.5)}$$

The angle θ_{HI} is given by

$$\cos\theta_{HI} = Y_I'/r_{HI} \quad . \qquad \text{(B.6)}$$

Substituting Y_I' from eq.(B.4) and (r_{HI}) from eq.(B.5) into eq.(B.6) gives the following

$$\cos\theta_{HI} = 0.6645$$

or $$\theta_{HI} = 48.36^0 \quad . \qquad \text{(B.7)}$$

Surname: PEEMOELLER Given Names: HARTWIG

Place of Birth: HAMBURG, GERMANY

Date of Birth: May 16, 1946

Educational Institutions Attended, with Dates of Entering and Leaving:

UNIVERSITY OF WINNIPEG 1966-1969

Degrees, Diplomas, Etc., Awarded, with Dates and Names of Institutions:

B.Sc. 1969 University of Winnipeg

Honors and Awards:

Publications:

Papers Presented at Scientific Meetings:

Sandhu, H.S. and Peemoeller, H. 1973. Nuclear spin-lattice relaxation in CH_2I_2 - CD_2I_2 mixtures. Bull. Am. Phys. Soc. 18, 1572.

PARTIAL COPYRIGHT LICENSE

I hereby grant the right to lend my thesis or dissertation (the title of which is shown below) to users of the University of Victoria Library, and to make single copies only for such users or in response to a request from the library of any other university, or similar institution, on its behalf or for one of its users. I further agree that permission for extensive copying of this thesis for scholarly purposes may be granted by me or a member of the University designated by me. It is understood that copying or publication of this thesis for financial gain shall not be allowed without my written permission.

Title of Thesis

Nuclear Magnetic Resonance Relaxation Time in CH_2I_2

Author [redacted]

Signature

HARTWIG PEEMOELLER

April 1974